Modeling the water and nutrient movement under biochar presence, slow-release fertilizer application and different water management, for two soil types during a rice column experiment in Cambodia

Auteur : Willemet, Rémy
Promoteur(s) : Degré, Aurore
Faculté : Gembloux Agro-Bio Tech (GxABT)
Diplôme : Master en bioingénieur : sciences et technologies de l'environnement, à finalité spécialisée
Année académique : 2021-2022
URI/URL : http://hdl.handle.net/2268.2/15500

LIÈGE université
Gembloux
Agro-Bio Tech

Modeling the water and nutrient movement under biochar presence, slow-release fertilizer application and different water management, for two soil types during a rice column experiment in Cambodia

REMY WILLEMET

THESIS PRESENTED FOR THE OBTAINING OF A DEGREE IN
BIOENGINEERING IN ENVIRONMENTAL SCIENCES AND TECHNOLOGIES

ACADEMIC YEAR 2021 - 2022

PROMOTER: Pr. AURORE DEGRE

LIÈGE université
Gembloux
Agro-Bio Tech

Modeling the water and nutrient movement under biochar presence, slow-release fertilizer application and different water management, for two soil types during a rice column experiment in Cambodia

REMY WILLEMET

THESIS PRESENTED FOR THE OBTAINING OF A DEGREE IN
BIOENGINEERING IN ENVIRONMENTAL SCIENCES AND TECHNOLOGIES

ACADEMIC YEAR 2021 - 2022

PROMOTER: Pr. AURORE DEGRE

This work was carried out within the Institute of Technology of Cambodia, in collaboration with the Cambodian Agricultural Research and Development Institute, and in line with Water-Soil-Plant Exchanges research axe of Gembloux Agro-Bio Tech faculty.
The Erasmus$^+$ organisation financed the student mobility.

Acknowledgememt

I would like to thank in the first place the host organisation and the people who accompanied me in this incredible experience. Prof. Ket, thank you for your guidance, your availability, your kindness and all these moments shared. Thank you Chenda for all your help and your time, you made me discover the Khmer culture in the best way possible. Arun, thank you for your support. Without forgetting Mengheak, Tola, Nachy, Vanntheng, Somnang, Sathea, Chanveasna, Sambath, Sophanith and Sna who made this trip unforgettable.

Un grand merci à Pr. Aurore Degré, dans un premier temps pour m'avoir donné l'opportunité de réaliser ce TFE rempli de découvertes. Dans un deuxième temps, pour votre disponibilité, votre agréable personnalité et votre expertise qui a su faire murir ma réflexion. C'était un réel plaisir de faire mon TFE sous votre encadrement.

Merci à toutes les personnes qui ont contribué de près ou de loin à surmonter cette épreuve. En commençant par ma partenaire d'aventure, Déborah. Mes compagnons de bureau Maya, Cédric et Romy. Tout le personnel de l'axe Eau-Sol-Plantes mais particulièrement les occupants du Topo. Le kot Néon's et ses habitants saugrenus. A mes relecteurs Anne-Catherine, Philippe et Myriam à la leather aiguisée. Et à toi Zoé, créatice de moments de bonheur.

Un merci particulier à mes camarades de STE et à ces personnes, qui même dans les moments difficiles, ont su apporter leur aide et prouver que Gembloux est bien plus qu'une université.

Merci à l'AG, au CB et au CRE d'avoir animé ma vie étudiante comme il se devait. On a pas eu le temps de s'ennuyer grâce à vous.

Mais le plus grand des mercis va à ma famille. A mes chers parents, pour m'avoir apporté un soutien indétrônable et pour avoir été des exemples tout au long de ma vie. Merci à mon grand-frère et ma grande-sœur d'avoir toujours été là pour moi et à leurs pièces rapportées qui font rayonner cette famille de leur présence. Sans oublier mes deux extraordinaires grands-parents, qui même la distance n'a pas réussi à faire pâlir leur soutien. Vous avez tous été les metteurs en scène de ma réussite

Abstract

Experimenting and developing accessible sustainable agricultural practices have become an economic and ecological major point in Cambodia. This study combines a modelling component with a soil column experiment testing biochar presence, slow-release fertilizer application, and alternate wetting and drying practices on two agronomically predominant soil types (Prateah Lang and Prey Khmer). Two thirds of water balance models were performed with high statistical indicators (NSE = 0,90; 0,98). The data input of the remaining third needs to be reviewed. For nutrient transport and transformation, it was possible to develop models with appropriate statistical indicators despite actual calibrated parameter values, by ignoring the dynamics of irrigation and multiple soil horizons. These models remain to be developed by the integration of concentration and leached amount of nutrient measurements still being processed. Parallel to this, the study highlighted several practices effects. Slow-release fertilizer positively impacts root length and plant height. Biochar improves root length, nutrient adsorption and Prateah Lang's hydraulic response, but seems to lead to the deterioration of Prey Khmer's texture. Alternate wetting and drying water practice system allows to increase root length without impacting plant height and seems to be diminishing water flow nutrient concentration. However, the sustainability of these approaches must be established. Indeed, it is important to take into account the economic and social aspects by considering yield and the workforce's accessibility to these technologies.

Keywords : Numerical modeling - HYDRUS-1D - Nutrient balance - Alternate wetting and drying - Slow-release fertilizer - Rice husk biochar

Résumé

Le développement de pratiques culturales durables et accessibles constitue une préoccupation économique et écologique importante au Cambodge. La présente étude s'intéresse à la modélisation d'une expérience en colonne de sol, intégrant l'utilisation de biochar et d'engrais à libération lente. Des méthodes d'humidification et de séchage alternées ont également été appliquées sur deux sols d'importance agronomique (Prateah Lang et Prey khmer). Il s'est avéré que deux tiers des modèles possèdent des indicateurs statistiques élevés au niveau de la balance hydrique (NSE = 0,90 ; 0,98). Les données d'entrées du tiers restant doivent être revus. Au niveau du transport et de la transformation des nutriments, il a été possible de développer des modèles aux indicateurs statistiques pertinents, malgré les valeurs erronées des paramètres calibrés. Par ailleurs, la dynamique de l'irrigation et la différenciation en horizons des sols n'ont pas été prises en compte. Ces modèles restent toutefois à perfectionner par l'intégration des mesures de concentration et de quantité lessivée de nutriments encore en cours de traitement. En parallèle, l'expérimentation a démontré les bénéfices des pratiques culutrales étudiées. Les engrais à libération lente ont des effets positifs sur la longeur racinaire et la hauteur des plantes. L'application de biochar améliore la longueur racinaire, l'adsorption des nutriments et la réponse hydraulique du sol Prateah Lang, mais détériore la réponse hydraulique du sol Prey Khmer. La méthode de mouillage et séchage alternée permet d'économiser de l'eau, tout en augmentant la longueur racinaire sans impacter la hauteur des plantes et semble diminuer la concentration des nutriments dans le flux d'eau. Cependant, la durabilité de ces pratiques doit être considérée. En effet, il est essentiel de prendre en compte les aspects économiques et sociaux en considérant le rendement et l'accessibilité de la main-d'œuvre à ces technologies.

Mots clés : Modélisation numérique - HYDRUS-1D - Bilan nutritif - Humidification et séchage alternés - Engrais à libération lente - Biochar d'écorce de riz

Table of contents

List of Figures

List of Tables

I Introduction

Rice production in Asia is responsible for 21 % of the global agriculture emissions (Jia et al., 2019). Besides, irrigation consumes 45% of the total freshwater in this part of the world (Cantrell, 2004). Tuong and Bouman (2003) predict that the south and south east of Asia will experience an "economic water scarcity" by 2025.

In Cambodia, agriculture accounts for a large share of employment representing up to 35,5% in 2019. Rice cultivation covers 64,5% of agricultural land, making it the main cultivated crop and a significant source of income for rural areas, where 87% of the population lives (CSES, 2020; GPCC, 2019). Natural resources are abundant and the agricultural work force is substantial in Cambodia (Kim et al., 2018). However, due to the yields and small harvested area, the nation's rice production and commercialisation lags below its potential, making it economically uncompetitive compared to Vietnam and Thailand (Kim et al., 2018; Bank, 2014). In 2016, Cambodia was the 12^{th} rice producer in the world with nine million tons of rice, behind Thailand and Vietnam at the 5^{th} and 7^{th} place with respectively 43 and 25 million tons of rice produced (Kea et al., 2019). According to "FAOSTAT" (2020), paddy rice yield in Cambodia is (37 568 hg/ha) higher than Thailand (29 064 hg/ha) but lower than China the leading producer (70 502 hg/ha) and Vietnam its direct neighbour (59 201 hg/ha). In addition, the Kingdom of Cambodia has the smaller harvested area (3000 ha) compared to Vietnam and Thailand (7000 and 10 000 ha).

Due to underdeveloped infrastructure, high production costs, climate change, low salaries and undertrained workers, Cambodia fails to reach its potential productivity (Cosslett & Cosslett, 2018). Resosudarmo and Chheng (2021) conclude that the poor reliable irrigation system (i.e. only 7% fully functional) is a significant cause of the lack of productivity but also of food insecurity in Cambodia. In addition, Kim et al. (2018) investigated climate change scenarios and concluded that improving irrigation is the most reliable technique to tackle the negative impact of increasing drought and flooding events.

Hence, there is therefore an economical and environmental challenge to find sustainable cultivation practices that combine emissions mitigation and water use improvement, through innovative practices and efficient use of fertiliser.

Paddy field is the common practice for rice cultivation in Asia. This technique describes a traditional rice-growing used on wetland soils with a prolonged submergence period coming from rainfall or irrigation (Witt & Haefele, 2005). The hydraulic conductivity of soils, and particularly the compacted horizon below the root system is the key for water management and cultural contaminants transport in the profile (Tan et al., 2015). This practice is nitrogen

and phosphorus limiting, leading to intensive use of fertiliser (Suriya-arunroj et al., 2000).

The most widely promoted water saving technique across the world to replace traditional continuous flood (CF) is the alternate wetting and drying (AWD) practice (Shekhar et al., 2017; Carrijo et al., 2017). Under AWD, the field is subjected to intermittent flooding and drying periods depending on a pre-defined threshold value of pounded water (i.e. soil moisture stress) and the state of development of the crop (Avil Kumar & Rajitha, 2019). The purpose of AWD is to minimise the threshold value in order to maximise water saving without compromising the yield, while taking into account the cultural conditions (Shekhar et al., 2017). However, the objective above is not simple to establish, as the literature reports different grain yields with AWD, including increase (Ye et al., 2013; Liu et al., 2013; LaHue et al., 2016), decrease (Lampayan et al., 2015; Xu et al., 2015) or without change (Linquist et al., 2015; Shekhar et al., 2020).

In addition, to enhance water use efficiency, there is a global mitigation of greenhouse gases (GHG) with AWD (Nabuurs et al., 2022). A change of anaerobic and aerobic conditions marks effects on electrochemical, chemical and microbial processes (Witt and Haefele, 2005; Ishii et al., 2011; Lüdemann et al., 2000). Yagi et al. (2020) mentioned that AWD induces a significant reduction of methane (CH_4) emissions, even if this mitigation may partly be offset by the promotions of nitrogen losses. Indeed, enhanced nitrate (NO_3^-) from nitrification of ammonium (NH_4^+) with aerobic conditions in the drying phase, can be easily denitrified to nitrogen (N_2) and nitrous oxide (N_2O) during a wetting phase (Tan et al., 2015). Instead, CH_4 production is reduced due to oxidation condition caused by drying periods, decreasing the activity of anaerobic bacteria (Yagi et al., 1997).

Besides water management, other innovative agriculture practices can be implemented, such as slow-release fertiliser (SRF) and biochar.
SRF releases nutrients at a slower rate than a conventional fertiliser by coated technologies reducing dissolution rate (Dong et al., 2016). Therefore, this is considered as a promising sustainable technology to mitigate nutrient losses, improve use efficiency use and reduce the costs and the time of application (Nardi et al., 2018; Dong et al., 2016). Studies show that SRF could reduce nitrogen volatilisation, surface runoff, leaching losses and increase total nutrient content at later stages (Chen et al., 2021; Jadon et al., 2018; Dong et al., 2016).
Biochar is an organic material produced by pyrolysis of organic matter (Lehmann et al., 2006). Several ranges of heating exist leading to different biochar varieties with distinct properties (Sohi et al., 2010). Its carbon stability allows it to persist in soil and present a strategic carbon sink in terrestrial systems (Lehmann et al., 2006; Singh et al., 2015). The structure of biochar induces a reduction of the bulk density, an improvement of soil water content and an increase of the total pore volume. These modifications change the available water capacity (AWC) as well as the hydro-physical properties of the soil peremptorily (Abel et al., 2013; Pratiwi and Shinogi, 2016; Das and Ghosh, 2017). Biochar also has chemical effects by increasing pH stability and improving cation exchange capacity (CEC) (Muhammad et al., 2018). These

improvements provide several side-effects such as developing microbial symbiotic interactions, nutrient use efficiency and physical plant response (Sohi et al., 2010; Al-Wabel et al., 2018). In addition to this hydro-physical and chemical changes, Yagi et al. (2020) reviewed the mitigation effects of biochar on GHG. It concluded that biochar reduces N_2O and CH_4 emissions and increases rice yields. However, fundamental mechanisms are not well understood due to biochar's multiple effects, application conditions and its different varieties (Yagi et al., 2020).

Determining the best agricultural practices through experiments is difficult, time consuming and expensive, especially with the addition of complex dynamics such as AWD, the presence of biochar and fertiliser rates. To deal with multi-factors interactions of water-soil-plant experiments, mathematical computer models could be considered as useful tools to understand and analyse physical, chemical and biological processes (Vereecken et al., 2016).

The purpose of this study is to create a model to assist in the sustainable governance of cropping practices. This study is integrated in a column experiment involving different water management, biochar presence, fertiliser application on two soil types. This model is based on measurements of irrigation, percolation, nutrient concentration, meteorological parameters and soil hydraulic parameters.

II Materials and methods

1 Field experiment and measurements

i Site description

The experiment was conducted in a greenhouse at the Cambodian Agricultural Research and Development Institute (CARDI) in Phnom Penh, from March to June 2022. The local altitude is 16m, with latitude 11°28'32.6"N and longitude 104°48'25.3"E. The Köppen's climate classification is Tropical Monsoon.

The greenhouse is composed of a glass panel roof and insect screens on the side walls. A black net was installed at 2,80m above ground level to reduce net radiation. The greenhouse is oriented North-South, continually ventilated by an aperture at the top and the screen walls, constructed with metal tubes and 10x5x4m chapel style (Figure 1).

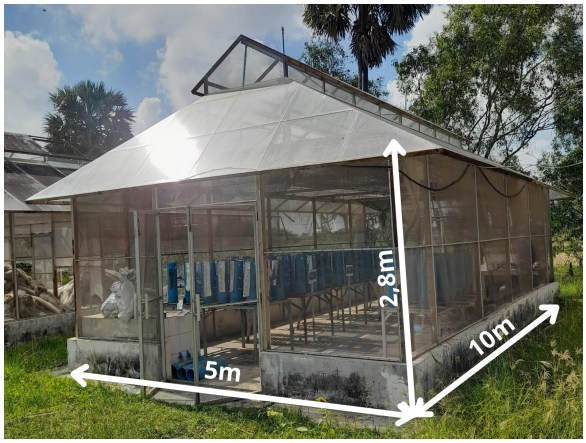

Figure 1: Experimental greenhouse

A weather station is located at 130m from the greenhouse, that includes wind speed, temperature, relative humidity, net radiation and precipitation sensors.

A second-class A evaporation pan was installed inside the greenhouse to estimate the potential evapotranspiration (ET_0).

ii Experimental design

The rice (*Oriza* L.) cultivar used was developed by the CARDI under the name *Sen Pidor*.

Several experimental conditions were considered during the rice column experiment such as :

- **Two soils were experimented** : Prateah Lang ($S1$) and Prey Khmer ($S2$) soils. They are located in the old colluvial-alluvial plains or the alluvial terraces and represent 40% of the rice-growing area in Cambodia (10-12% Prey Khmer; 25-30% Prateah Lang)(Figure 2)

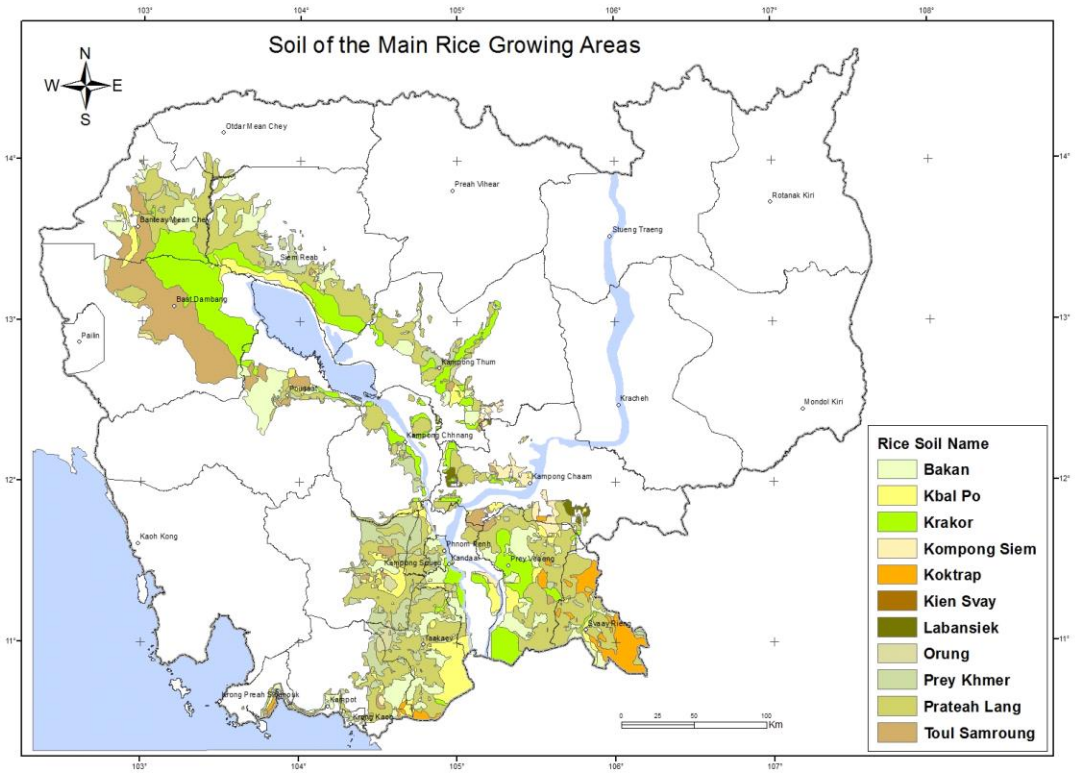

Figure 2: Cambodia's soil map of the main rice-growing areas (White et al., 1997)

Prateah Lang is a clay soil and Prey Khmer a sandy-loam soil according to the USDA textural triangle. These two soils are composed of three horizons each (Appendix B). The physical and chemical analysis of the soils are shown in Table 1.

Table 1: Chemical and physical parameters of the two soils. CEC is the cation exchange capacity, SOC and SOM represent soil organic carbon and matter respectively, EC refers of the electric conductivity

Parameters	**Prateah Lang S1 (Clay)**			**Prey Khmer S2 (Sandy-Loam)**		
Depth of analysis	**0-20cm**	**20-40cm**	**40-60cm**	**0-20cm**	**20-40cm**	**40-60cm**
% sand	23,5	19,5	16,8	74,5	68	55
% silt	24,1	23,1	11,7	21	22,5	32,6
% clay	52,4	57,4	71,5	4,5	9,5	12,4
Bulk density $[g/cm^3]$	1,42	1,55	1,72	1,34	1,38	1,55
pH	5,027	5,127	5,627	6,417	6,080	6,120
CEC $[cmol/kg]$	1,23	1,34	2,89	0,88	0,92	1,13
SOC [%]	2,635	2,347	2,263	0,147	0,178	0,131
SOM [%]	3,089	2,751	2,654	0,172	0,209	0,154
Total N $[g/kg]$	1,96	2,11	0,67	1,12	0,62	0,93
Available P $[mg/kg]$	20,5	12,5	14,89	1,6	0,95	1,12
Echangeable K $[cmol/kg]$	0,15	0,09	0,06	0,08	0,05	ND
EC $[uS/cm]$	23,347	28,227	28,763	33,270	34,15	35,463

- **Two water management practices** : continuous flood (CF) and alternate wetting and drying (AWD). In CF practice, a ponded layer of water is maintained over the field during

the entire rice growing period. In AWD, a water-saving practice, the field is subjected to a cycle of a flooding period followed by a drying period (until ponded water reaches -15cm below ground).

- **Biochar impacts** : the application in the plough layer of biochar of 4t/ha and 6t/ha concentrations was taken into account, as well as a control column. The biochar is produced from the rice husk pyrolysis and its first analysis is shown in Table 2.

Table 2: Biochar chemical and physical parameters

pH	ECE [uS/cm]	Bulk density [$g/cm3$]
8.91	0,456	0,79

- **Nutrient application** : on March 22nd and April 26th 2022, SRF was applied. The concentration used was 300kg/ha of NPK 60:30:30, representing 0,3186g of N (15% of NH_4^+ and 85% of NO_3^-) and 0,1062g of P and K divided in two applications, as recommended by the host institute (CARDI).
- **Three stages of development** : destructive measurements (explained in section iii) were carried out at the first three stages of development of the crop : tillering (49 days), boosting (79 days) and flowering (98 days). The short duration of the experiment prevented the plant from reaching complete maturity.
- **Three repetitions of each parameters**.

In total, 36 undisturbed column samples for $S1$ and 72 for $S2$ were required to fulfil all the experimental conditions. An incident (Appendix A) reduced the total number of columns to 97. In consequence, some experimental replications were suspended as shown in the experimental plan (Figure 3). To simplify the comprehension of this document, the combination of biochar and SRF is categorized into 4 treatments. Treatment zero corresponds to a column without SRF and without biochar, treatment one with SRF and without biochar, treatment two with SRF and with 4 t/ha of biochar, and treatment three with SRF and with 6 t/ha of biochar.

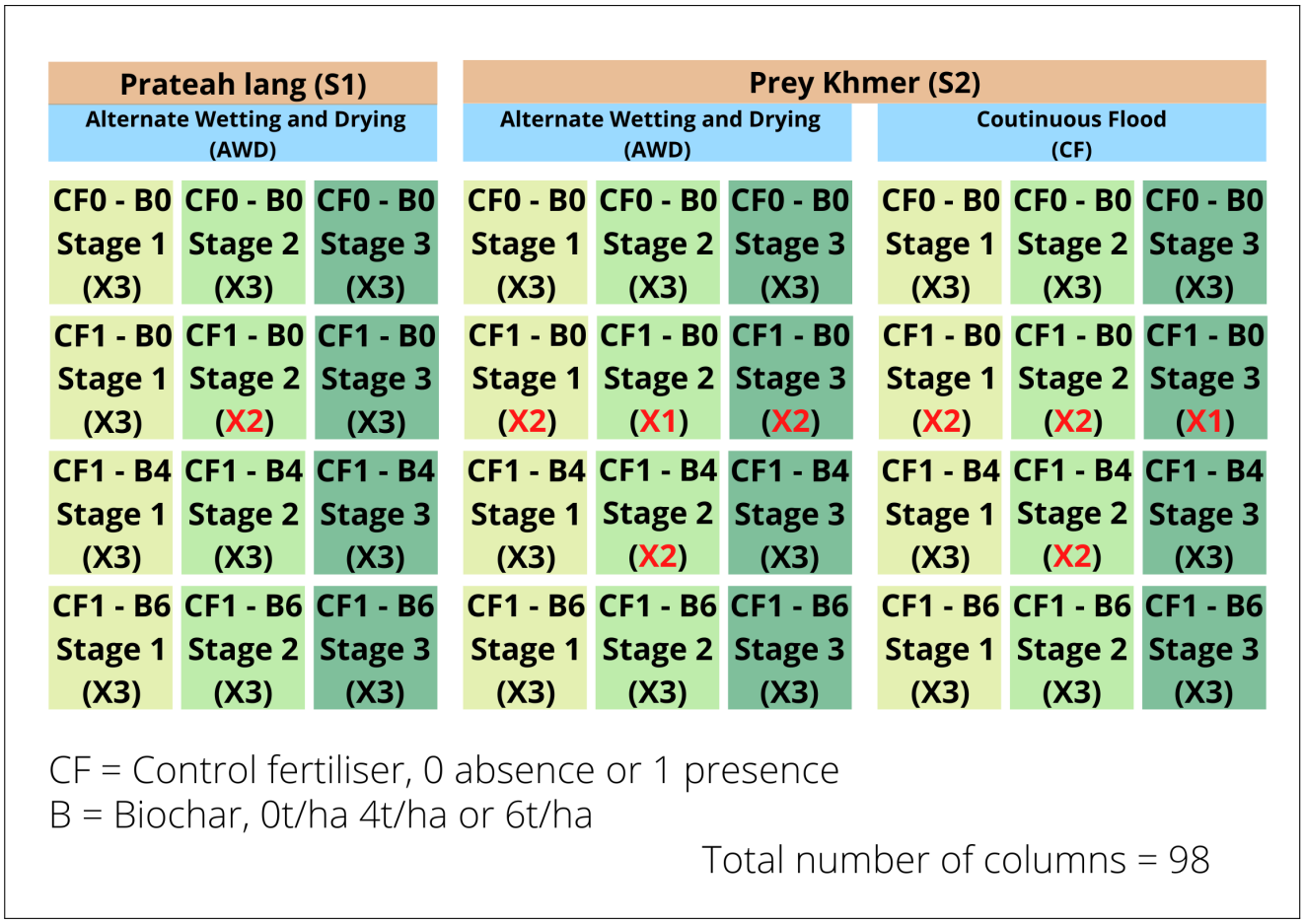

Figure 3: Experimental plan for the two different soils according to water management practices, growth stage and fertilizer application

Each column corresponds to a PVC tube with a height of 60cm and a diameter of 15cm. Two valves to collect running water samples were added at a height of 20 and 35cm from the bottom of the column. A third valve was installed at the bottom to help saturate the column before the start of the experiment. During the experiment, atmospheric conditions were applied at the bottom by letting the valve open. Figure 4 represents the column experiment according to the two soil profiles (Appendix B).

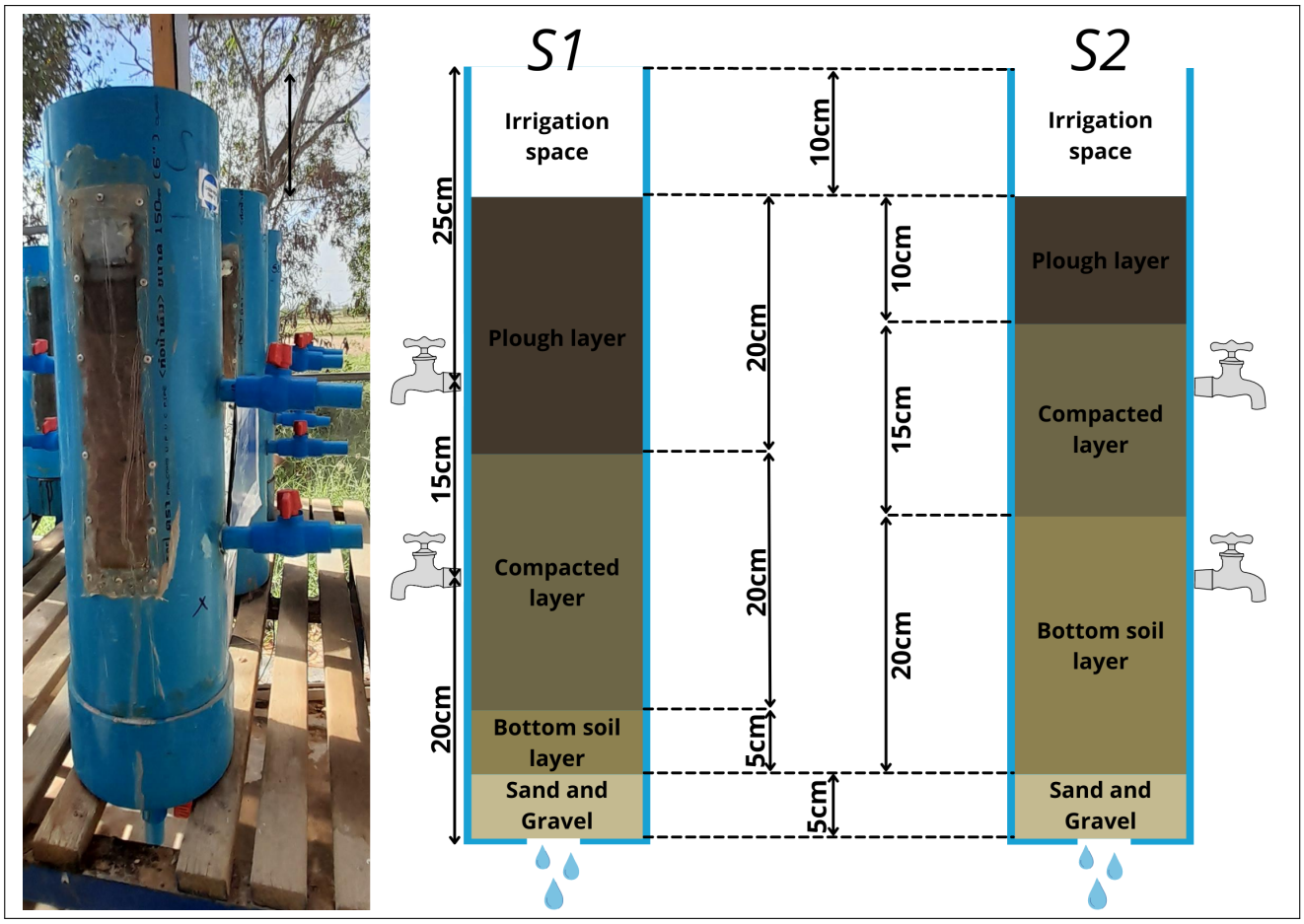

Figure 4: Representation of the experimental column according to the Prateah Lang (S1) and Prey Khmer (S2) soil profiles

iii Experimental measurements and analysis

For each horizon, the hydraulic conductivity at saturation (K_s) and the water retention curve (WRC) were determined. A first sampling campaign on the field was realised for the three layers of S1 and for the first layer of S2. A second one was conducted after 49 days of experimentation for the two deeper layers of S2 and for the first layers of each soil containing the two rates of biochar. To measure K_s, a KSAT device (KSAT, METER Group) was used in the first campaign and a handcrafted constant head device (Appendix D) for the rest of the samples.

Pressure plate experimentation was used on the two sampling campaigns to determine the WRC.

The WRC is a representation of water content change depending on tension applied by the soil. The transfer of water from the soil into the roots is possible when the plant is able to overcome the tension applied by the soil to the water. To simplify the understanding of the results, the tension in the soil is presented as the logarithm of a positive value called pF. A value of pF=1 corresponds to saturated conditions and its increase represents drying conditions.

Derivatives of water content (θ) by matrix tension (h) combined with Jurin's law were realised to represent pore size frequency against radius pore size (Kutilek et al., 2007).

Jurin's law (representation of capillary rise as a function of tube diameter) applied to soil provides a relation between tension and pore radius (i.e. at a given tension, water fills pores with a minimum radius size) :

$$h = \frac{2\gamma \cos\theta}{r\rho g} \Rightarrow r = \frac{1,5}{h} \tag{1}$$

Where h is the matrix tension in cm (L); γ is the surface tension of water at $20°C$ (MT^{-2}); θ is the contact angle assumed to be equal to 0 (-); r is the pore radius in mm (L); ρ is the density of pure water (ML^{-3}); g is the gravity constant (LT^{-2}).

During the experimentation physical and chemical measurements were taken :

- Volumetric amount of percolated water at seven-day intervals
- Volumetric amount of input water
- Evaporation of the pan class A
- Nutrient concentration at the two control points at seven-day intervals
- Nutrient concentration of percolated water
- Leaf area index (LAI) at the three stages of development
- Plant height at seven days intervals
- Root length at the three stages of development

LAI represents the area of one side of the leaves per unit area of ground [-] (Monteith & Unsworth, 1990). The Petiole Pro plant leaf area meter app (version 1.4.15[1]) was used to measure the cumulative surface of leaves for every column during every stage of measurement (Appendix C). The ground surface was taken as the exposed soil surface of the column equal to $0{,}071m^2$.

iv Statistical analysis

An anova one-way statistical analysis was performed for the various treatments (biochar and fertilizer) and soils combined with water management. Sampling was considered to be random, simple and independent. Variance equality was calculated with a Levene test. The normality of the populations was tested with a Shapiro-Wilk test for measurement with more than 10 observations by modality. The normality was assumed for the rest. To examine the mean difference, a Tukey honest test was realised for the parametric population and a Dunn's test for the non-parametric one.

[1] https://petioleapp.com

2 HYDRUS-1D model

Figure 5 summarizes the processes presented in this section.

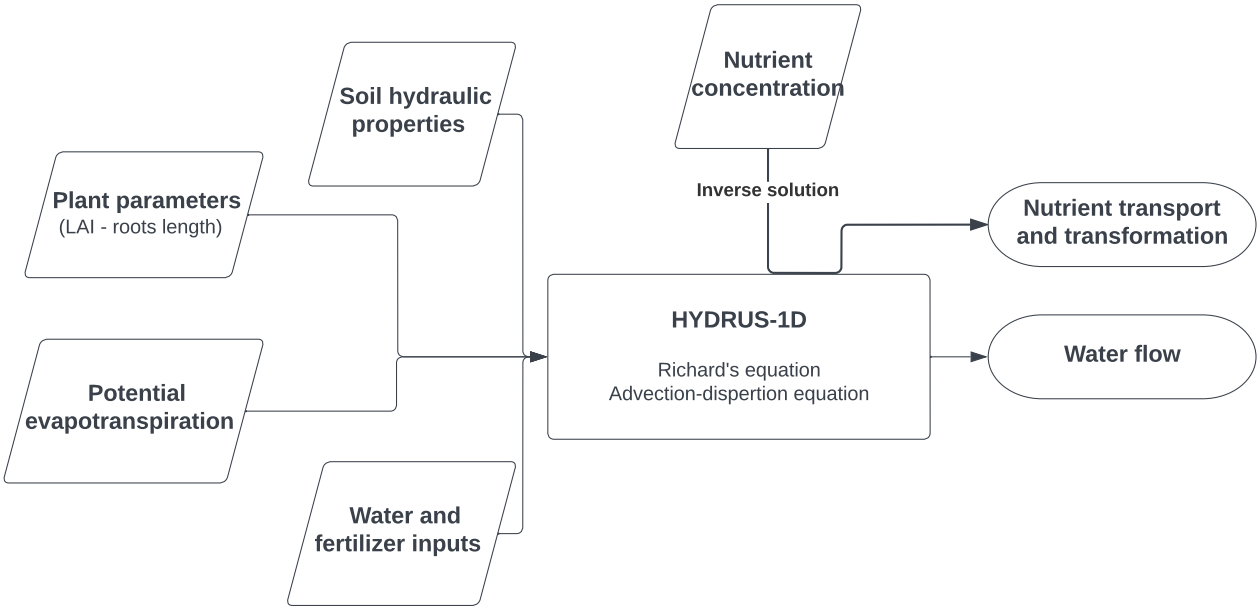

Figure 5: Flowchart outlining the experiment's modeling approach

i Model description

Šimůnek et al. (2013) reviewed relevant models approach for water and nutrient cycling, in which the most advanced models used are the Richards equation and convection-dispersion equation respectively. Many studies show the accuracy of these mathematical computer models to represent percolation and/or transport cultural contaminants in the vadoze zone under different water management during rice crop experiments (Li et al., 2015; Tan et al., 2015; Shekhar et al., 2021b; Jyotiprava Dash et al., 2015; Yang et al., 2017; Mo'allim et al., 2018; Jha et al., 2017). To represent water, nutrient, plant growth and heat transport under saturated and unsaturated conditions, various software exist such as HYDRUS, Soil–Water–Atmosphere–Plant (SWAP) or MACRO-5.2 for example.

The HYDRUS-1D model software (pc-progress) was selected to simulate the experimentation because it proved its efficiency in several studies (Bahmani et al., 2019; Chowdary et al., 2004; Gupta et al., 2021; Li et al., 2015; Shekhar et al., 2021a; Tan et al., 2015; Yang et al., 2017) and offers an inverse model option to calibrate hydraulic and physico-chemical model parameters. "The method was found to be very effective and has become a standard in non-linear least-squares fitting among soil scientists and hydrologists" (Šimůnek et al., 2013).

ii Model parameters

Water flow movement

The governing 1-D flow program solves the modified Richard's equation numerically for water flows (Equation 2). The effect of air phase and thermal gradients can be neglected in the water flow process (Šimůnek et al., 2013).

$$\frac{\delta\theta}{\delta t} = \frac{\delta}{\delta x}[K(h)(\frac{\delta h}{\delta x} + 1)] - S \tag{2}$$

Where θ is the volumetric water content (L^3L^{-3}); t is the time variable (T); x is the spatial coordinate (L) ; h is the water pressure head (L); S is the sink term ($L^3L^{-3}T^{-1}$); $K(h)$ is the unsaturated hydraulic conductivity function (LT^{-1}).

The water flow model was simulated using the measurements of percolated water, evaporation, transpiration and irrigation for CF and AWD.

Soil hydraulics properties

The soil water retention $\theta(h)$ and hydraulic conductivity $K(h)$ functions according to Van Genuchten (1980), are given as:

$$\theta(h) = \begin{cases} \theta_r + \frac{\theta_s - \theta_r}{[1+(\alpha h)^n]^m} & h < 0 \\ \theta_s & h \geq 0 \end{cases} \tag{3a}$$

$$K(h) = K_s S_e^l [1 - (1 - S_e^{1/m})^m]^2 \tag{3b}$$

Where θ_s is the saturated water content (L^3L^{-3}); θ_r is the residual water content (L^3L^{-3}); m, α and n are empirical shape factors (-); K_s is the saturated hydraulic conductivity (LT^{-1}); l is the pore-connective factor in the hydraulic conductivity function (-); Se is the relative saturation (L^3L^{-3}).
Se, m and n are defined as follows :

$$Se = \frac{\theta - \theta_r}{\theta_s - \theta_r} \quad \text{and} \quad m = 1 - \frac{1}{n} \tag{4}$$

The pore connective parameter l is equal to 0,5 on average (Mualem, 1976) and K_s was measured (section iii).

Evaporation and transpiration

Potential evapotranspiration (ET_0), which incorporates the various effects of the weather conditions, is needed to estimate daily soil evaporation and plant transpiration. ET_0 was

established on pan evaporation measurement by the equation (Allen et al., 1998) :

$$ET_0 = K_p \times E_{pan} \tag{5}$$

Where ET_0 is the potential evapotranspiration (L); K_P is the pan coefficient (-); E_{pan} is the daily evaporation (L).

K_P is related to wind speed, relative humidity and size of the border crop (Allen et al., 1998). The relative humidity and wind speed were taken from the weather station due to the impossibility of measuring them inside the greenhouse. This assumption was supported by two observations :

- Experimental conditions inside the greenhouse were close to the weather station. The greenhouse was permeable to wind and humidity. In addition, the weather station was in a closely comparable environment
- Allen et al. (1998) provides K_p coefficients depending on large ranges of values

As a consequence of a lack of daily measurements, the missing data of E_{pan} was completed by a linear relation of ET_0 calculated by the Penman-Monteith equation (Allen et al., 1998) from the weather station.

The evapotranspiration under standard conditions (ET_C) was calculated by the crop coefficient approach (Allen et al., 1998) :

$$ET_C = ET_0 \times K_C \tag{6}$$

Where ET_C is the crop evapotranspiration (LT^{-1}); ET_0 is the potential evapotranspiration (LT^{-1}); K_C is the crop coefficient (-).

The K_C value varies with the type of crop and its state of development. K_c for paddy rice was taken from Allen et al. (1998) and corresponds to 1,05, 1,20 and 0,75 for tillering, boosting and flowering growth stages respectively.

Potential evaporation and transpiration are estimated depending on crop development stages (Belmans et al., 1983) :

$$E_P = ET_C \times e^{Kgr*LAI} \tag{7a}$$

$$T_P = ET_C - E_p \tag{7b}$$

Where E_P and T_P are evaporation and transpiration (LT^{-1}); ET_C is the crop evapotranspiration (LT^{-1}); Kgr is an extension coefficient for global solar radiation (-); LAI is the leaf area index (L^3L^{-3}).

Kgr is taken as 0,3 for rice crop (Phogat et al., 2010).

Root Growth

The root growth is represented in HYDRUS-1D by a Verhulst-Pearl logistic growth model (Šimůnek & Suarez, 1993). The root depth (L_r) evolution during the experiment is calculated by :

$$L_r(t) = L_m \times f_r(t) \tag{8}$$

Where L_r is the root depth (L); L_m is the maximum root depth (L); f_r is the Verhulst-Pearl logistic growth coefficient (-); t is the time variable (T).

f_r is calculated from Equation 9 and was calibrated for the different experimental conditions by the root growth stage measurements.

$$f_r(t) = \frac{L_0}{L_O + (L_m - L_0)e^{-rt}} \tag{9}$$

Where L_0 is the initial root depth (L); L_m is the maximum root depth (L); r is the growth rate (T^{-1}); t is the time variable (T).

Root water and nutrient uptake

In Richard's equation (Equation 2), the sink term (S) represents the water removed from the soil by the roots over time. HYDRUS-1D takes into account the roots water uptake by using the Feddes water stress function (Feddes, 1982) :

$$S(h) = \alpha(h) \times S_p \tag{10}$$

Where S is the roots water uptake ($L^3L^{-3}T^{-1}$); α is the water stress function; S_p is the potential roots water uptake rate ($L^3L^{-3}T^{-1}$); h is the soil matric potential (L).

The stress water function ($\alpha(h)$) is a dimensionless function taking value between zero and one, determined by the water stress due to soil matric potential (i.e. water pressure head) and the potential evaporation.

The stress factor is assumed to be zero at the wilting point ($h < h4$) and in saturated condition ($h > h1$). The optimal zone is in the range of $h2$;$h3$, and the response the stress response decreases (increase) linearly between $h3$;$h4$ ($h1$;$h2$). The function is limited between two values of potential transpiration, the lowest value ($r3_l$) fixed at 0,1cm/day and the upper value ($r3_h$) fixed at 0,5cm/day (Figure 6).

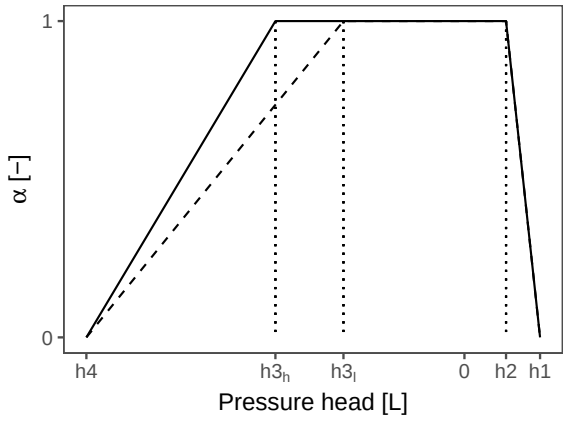

Figure 6: Stress response function according to Feddes (1982)

The stress response is interpolated between these two values of potential transpiration (Šimůnek et al., 2013) :

$$h3 = \begin{cases} h3_l & r3_l \geq T_P \\ h3_h + \frac{(h3_h - h3_l)}{(r3_l - r3_h)} * (r3_h - T_p) & r3_l < T_p < r3_h \\ h3_h & r3_h \leq T_P \end{cases} \tag{11}$$

Singh et al. (2003) optimised the Feddes' parameters for rice culture: $h1 = 100\ cm$,$h2 = 55\ cm$, $h3_h$ =-160 cm, $h3_l$ =-250 cm, and $h4$ =-15 000 cm. Positive value of $h1$ allows to consider the submerged rice crop.

By introducing a non-uniform distribution coefficient ($b(y)$) integrated to unity over the vadoze zone, the potential water uptake rate (S_p) (i.e. the potential transpiration rate per depth of the root zone) is generalised (Šimůnek et al., 2013) :

$$S_p(y) = T_p \times b(y) \tag{12a}$$

$$\int_{L_r} b(y)dy = 1 \tag{12b}$$

Where S_p is the potential water uptake (TLL^{-1}); T_p is the potential transpiration rate (LT^{-1}) (Equation 7b); b is the normalised water uptake (L^{-1}); L_r is the root depth (L); y is the vertical component (L).

Hoffman and Van Genuchten (1983) established an arbitrary trapezoid shape for the distribution coefficient resumed in HYDRUS-1D when rooting depth varies in time (Šimůnek et al., 2013), governed by :

$$b(y) = \begin{cases} \frac{1.667}{L_r} & y > L - 0,2L_r \\ \frac{2.0833}{L_r}(1 - \frac{L-y}{L_r}) & L - L_r < y < L - 0,2L_r \\ 0 & y < L - L_r \end{cases} \tag{13}$$

Where L is the y coordinate of the soil surface (L); L_r is the root depth (L).

The nutrient uptake approach depends on the root depth and the plant transpiration. It was considered only in a passive way. The passive way is performed by the movement of dissolved nutrients coupled with the root water uptake. A maximum limit concentration is needed in HYDRUS-1D, and was set at $1000mg/l$ (Yang et al., 2017). This value is above the concentrations possibly encountered in this experiment.

Nutrient transport and transformation

The solute transport in the vadoze zone is based on the advection-dispersion equation (Šimůnek et al., 2013). It requires parameters as diffusion coefficients in free water (D_w), in air (D_a) and longitudinal dispersivity (D_L). The dispersion coefficient in the liquid phase (D) is given by Bear (1988) :

$$\theta D = D_L|q| + \theta D_w \tau_w \tag{14}$$

Where D is the dispersion coefficient (L^2T^{-1}); D_L is the longitudinal dispersivity (L); q is the flux density (LT^{-1}); D_w is the molecular diffusion coefficient (L^2T^{-1}); τ_w is the tortuosity factor (-) calculated by the relationship of Millington and Quirk (1961) :

$$\tau_w = \frac{\theta^{7/3}}{\theta_s^2}\tau_g = \frac{a_v^{7/3}}{\theta_s^2} \tag{15}$$

Where τ_w is the tortuosity factor in liquid and gas phases (-); a_v is the air content by volume of soil (L^3L^{-3}); θ_s is the water content at saturation (L^3L^{-3}); θ is the water content (L^3L^{-3}).

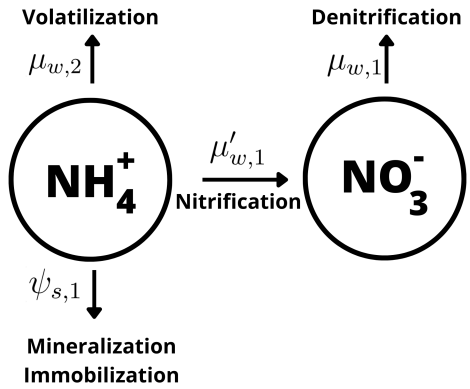

Figure 7: Nitrogen decay chain representation

The solute transformation model of nitrogen for this experiment takes several processes into consideration : nitrification ($\mu'_{w,1}$), volatilization ($\mu_{w,1}$), denitrification ($\mu'_{w,2}$), mineralization/ immobilization ($\psi_{s,1}$). w and s represent the liquid and solid phases. μ processes are considered to be a first-order rate reaction and ψ process a zero-order rate reaction. $'$ indicates the connection between the different N species noted 1 and 2 corresponding to NH_4^+ and NO_3^- respectively (Šimůnek et al., 2013; Tan et al., 2015; Li et al., 2015; Shekhar et al., 2020).

The partial differential equations are used to represent the one-dimensional first-order decay chain reaction during saturated and unsaturated transient water flow. The decay chain reaction based on Šimůnek et al. (2013) is shown in Equation 16 and represented in Figure 7.

The phosphorous dynamic modeling doesn't take into consideration decay chain reaction. The advection-dispersion equation for a one-dimensional soil profile takes a simpler form as shown in Equation 17 (Shekhar et al., 2021a).

Nitrogen :

$$\frac{\delta\theta C_{w,1}}{\delta t} + \frac{\delta c_{s,1}}{\delta t} = \frac{\delta}{\delta z}(\theta D_{2-1}\frac{\delta C_{w,1}}{\delta z}) - \frac{\delta q C_{w,1}}{\delta z} - (\mu'_{w,1} + \mu_{w,1})\theta C_{w,1} + \gamma_{s,1}\rho - r_{a,1} \quad (16a)$$

$$\frac{\delta\theta C_{w,2}}{\delta t} = \frac{\delta}{\delta z}(\theta D_2\frac{\delta C_{w,2}}{\delta z}) - \frac{\delta q C_{w,2}}{\delta z} + \mu'_{w,1}\theta C_{w,1} - \mu_{w,2}\theta c_{w,2} - r_{a,2} \quad (16b)$$

Phosphorous :

$$\frac{\delta\theta C_w}{\delta t} = \frac{\delta}{\delta z}(\theta D\frac{\delta C_w}{\delta Z}) - \frac{\delta q C_w}{\delta z} - r_a \quad (17)$$

Where C is the nutrient concentration (ML^{-3}); ρ is the soil bulk density (ML^{-3}); D is the dispersion coefficient (L^2T^{-1}) (Equation 14); q is the volumetric water flux (LT^{-1}); r_a is the root nutrient uptake ($ML^{-3}T^{-1}$); μ and γ are transformation rate constants (T^{-1}).

To represent the adsorption, a one-site kinetically controlled sorption with a linear isotherm equation was chosen. This allows to represent preferential flow by considering the adsorption between solid phase and liquid concentration as not instantaneous (Šimůnek et al., 2013; Rassam et al., 2018):

$$\frac{dS}{dt} = \alpha(\frac{K_d C^\beta}{1 + \eta C^\beta} - S) \quad (18)$$

Where S is the concentration in the solid phase (MM^{-1}); C is the liquid concentration (ML^{-3}); K_d is the distribution coefficient (L^3M^{-1}); α is a first order rate coefficient (T^{-1}), η (L^3M^{-1}) and β (-) are Langmuir and Freundlich isotherm parameters, equal to zero and one respectively to represent a linear sorption.

The concentration of the three modelled chemical species is related to the experimental conditions. To represent SRF, a first-order degradation rate over 10 days was taken.

iii Model calibration and validation

Calibration

A calibration of parameters for water flow movement and nutrient transport/transformation was carried on by an inverse solution in HYDRUS-1D with two-thirds of the data set. The one-third of the data remaining was used as validation. For experimental conditions that had a reduced number of column (Appendix A), the data were separated in two in the case of two columns remaining and repeated in the case of one column remaining, between calibration and validation datasets.

The calibration used the Marquardt-Levenberg algorithm to represent the experimental

conditions on the model's parameters. This algorithm minimizes the objective function (θ) by combining the Newton and steepest descent methods (Hopmans et al., 2002; Šimůnek et al., 2018).

$$\theta(b, y) = \sum_{j=1}^{m_y} v_j \sum_{i=1}^{i=n_j} w_{i,j}[y'_j(z, t_i) - y_j(z, t_i, b)]^2 \tag{19}$$

Where y_j and y_j' are model prediction and measured respectively; b is the optimized soil hydraulic or/and solute transport/transformation parameters; m_y is the number of measurement types; n_j is the number of measurements for a certain type of measurement j; w and v are weighting factors.

A representation of the simulation inverse for water flow is given by Hopmans et al. (2002) (Figure 8). This representation also works for nutrient processes, the "outlflow rate, Matric head" is transformed into "nutrient concentration" and "Soil hydraulic models" into "Solute transport and transformation models".

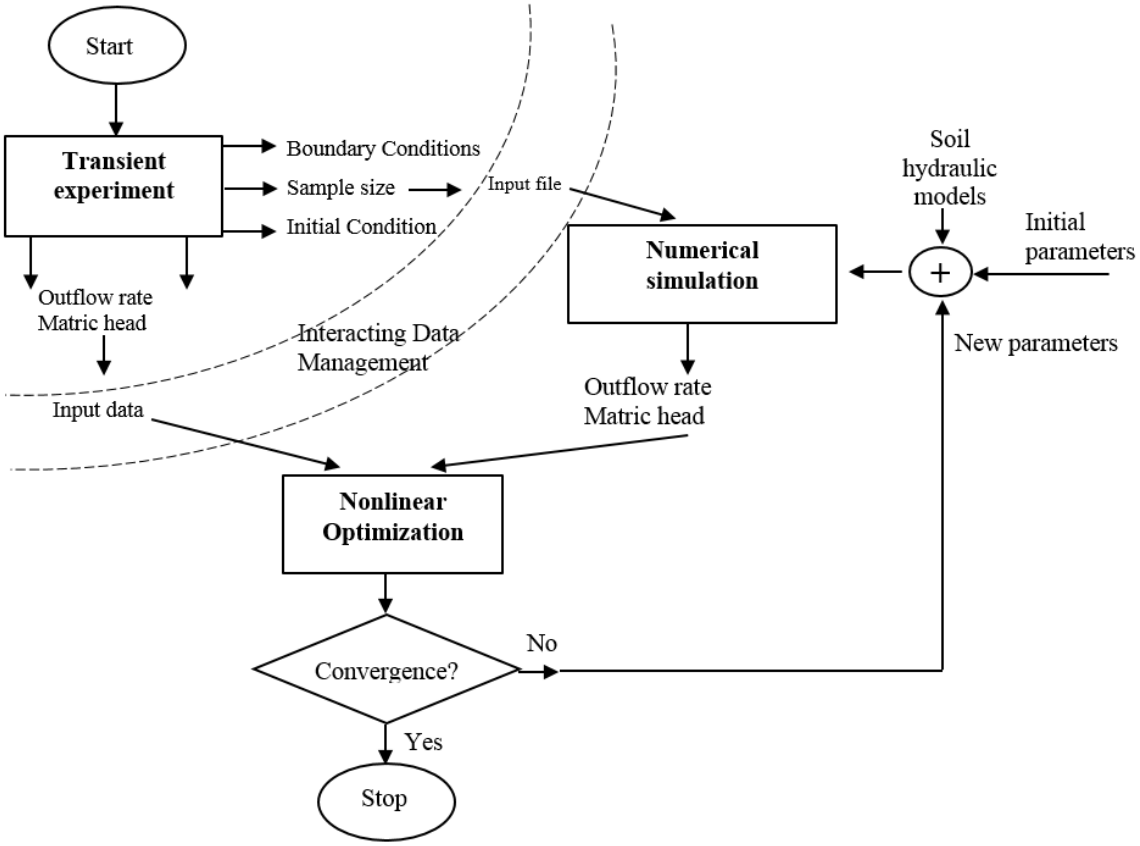

Figure 8: Inverse modeling method procedure (Hopmans et al., 2002)

Water movement

Based on pressure plate measurements, four of the seven Van-Genuchten parameters remaining (θ_S; θ_r; α; n in Equation 3a) were calibrated for the two soil types with three layers and the presence or lack of biochar thanks to RETC. This program, used to quantify the hydraulic function of unsaturated soils, employs a non-linear least-squares optimization approach (Van Genuchten et al., 1991).

Solute transport and transformation

Three inorganic solutes were represented, Nitrate (NO_3^-), Ammonium (NH_4^+) and Phosphate (PO_4^{3+})

In the solute transport, diffusion in air (D_a) is neglected due to its low impact and diffusion in water (D_w) was initially set at 1,52, 1,64 and 0,53 cm^2/day for $NH4^+$, $NO3^-$ and PO_4^{3-} respectively (Li et al., 2015; Rassam et al., 2018). D_L was initially fixed at one-tenth of the height of the experimental depth profile (Lallemand-Barres and Peaudecerf 1978, cited in Gupta et al., 2021; Freiberger et al., 2018).

For solute reactions, it is complicated to find parameters for decay chain reactions using laboratory or field experiments (Shekhar et al., 2021b).

For chain reaction calibration, the initial values for nitrogen transformation rate constants were referred to the range given in Tan et al. (2015). Immobilization only in the root-zone (0-40cm) (Li et al., 2015). For phosphorous (PO_4^{3-}), initial values were based on Freiberger et al. (2018).

Due to anionic charge, the distribution coefficient (K_d) of NO_3^- was not considered for solute isotherm adsorption. 3,5 cm^3/g and 3,12 cm^3/g values were taken as adsorption initial values for NH_4^+ and PO_4^{3-} respectively (Lotse et al., 1992; Shekhar et al., 2021a).

All these solute transport and reaction parameters were implemented in HYDRUS-1D, and nutrient concentration measurements from the different control nodes were used to calibrate these parameters.

Validation

The validation was performed on water percolation and nutrient concentration measurements. As recommended in Moriasi et al. (2007), Nash-Sutcliffe modeling efficiency (NSE) and percent bias (PBIAS) were used to describe the water and nutrient models' performance, respectively.

The PBIAS method calculates the average tendency of the simulated data to differ from the observed data in either direction. Positive values indicate underestimation and negative values overestimation (Gupta et al., 1999) (Equation 20a).

The Nash-Sutcliffe efficiency (NSE) is a normalised statistic that assesses the proportion of residual variance (i.e. noise) to measured data variance (i.e. information) (Nash & Sutcliffe, 1970) (Equation 20b).

$$PBIAS = \frac{\sum_{i=1}^{n}(O_i - P_i) * 100}{\sum_{i=1}^{n}(P_i)} \tag{20a}$$

$$NSE = 1 - \frac{\sum_{i-1}^{n}(O_i - P_i)^2}{\sum_{i-1}^{n}(O_i - \overline{O})^2} \tag{20b}$$

Where P_i is the predicted value; O_i is the observed value; n is the number of data pairs; p is the number of parameters estimated during optimization; $\overline{O}$ is the observed mean value.

The Table 3 below reports the value of the performance ratings for the monthly time step.

Table 3: Ratings of general performance for suggested statistics for a monthly time step (Moriasi et al., 2007)

	NSE	PBIAS %
Very good	]0,75; 1]	[0; 25[
Good	]0,65; 0,75]	[25; 40[
Satisfactory	]0,50; 0,65]	[40; 70[
Unsatisfactory	[-∞; 0,50]	[70; 100]

iv Initial and boundary conditions

The initial soil moisture conditions were assumed to be near the saturation (i.e. matric potential equal to -100cm) in the entire profile.
The initial solute concentrations of NH_4^+, NO_3^- and PO_4^{3-} were fixed depending on the chemical analysis of soils (Table 1).

A daily time step was taken. The atmospheric boundary condition with a surface layer to account for evaporation, irrigation, fertilization and a maximum pounded water surface set at 15cm was taken. The bottom condition was settled with "Seepage face=0", allowing the representation of column experiments with the bottom exposed to the atmosphere.

For the nutrient transport process, a Gauchy type (third type) and a Drichlet type (first type) were employed for the surface and bottom boundary conditions respectively (Yang et al., 2017; Tan et al., 2015; Shekhar et al., 2020). Gauchy represents solute flux and Dirichelt solute concentration (Šimůnek et al., 2013).

III Results and discussion

1 Retention and porosity curves

The WRC based on pressure plate experiments and the derived porosity curves are shown in Figures 9 and 10. Porosity curves are a representation of the variation of water content associated with porosity assumption size. It is not representing the real soil porosity, but an estimation based on WRC.

Porosity can be defined into macro and micro porosity, but the limitations and number of classes may vary depending on the literature. In this study, the limit between these porosities is fixed at 0,05mm diameter (pF = 1,78) (Kiehl, 1979 cited by Stolf et al., 2011). At this limit, macroporosity depends on texture and bulk density (impacted by the structure) and the microporosity mainly on texture (Stolf et al., 2011). AWC is observable between the field capacity (pF = 2,5) and the wilting point (pF = 4,2) (Giap et al., 2021).

i Soil comparison

Prateah Lang soil (S1) shows similar water content at saturation equal to 0,30, 0,34 and 0,33cm^3/cm^3 in the first, the second and the third horizon respectively. The residual water content is similar to the first and second horizon (0,12, 0,10cm^3/cm^3) but increases in the third (0,20cm^3/cm^3). α and n shape parameters show comparable values to the three horizons leading to a similar retention curve shape (Figure 9a(1)). The conductivity of the first, second, and third horizons at saturation are 0,58, 29,75 and 38,04 cm/day, respectively.

The difference in residual water content values is due to the microporosity influenced by the texture. The first two horizons contain around 50% of clay compared to 70% in the last one, retaining more water against higher tension. The conductivity at saturation for the first horizon is relatively low compared to the literature (15cm/day) (Poulton et al., 2015).

Prey Khmer soil (S2) possesses residual water content in a close range of values increasing with depth (0,15, 0,16, 0,18cm^3/cm^3). The second horizon contains less water at saturation (0,25cm^3/cm^3) than the first and the third one (0,39, 0,41cm^3/cm^3). Shape parameters are different for α (0,03, 0,00, 0,10) and are equivalent for n ($\approx$ 1,54). The conductivity at saturation is different between the three horizons, with 19,44, 38,04 and 3,24 cm/day in the first, second and third respectively.

Similarly to S1, the residual water content values of S2 increase with depth, such as clay and silt content. The variation of the Van Genuchten parameters for the second horizon leads to a retention curve with a smaller amplitude and a water content lower in the macroporosity as shown in Figure 10a(1). Because macroporosity is affected by soil structure, tillage practices may have unstructured this horizon.

However, this hypothesis is not corroborated with the depth of the horizon (not deep enough for traditional ploughing) and with the bulk density being similar to the first horizon (1,34 and 1,38 g/cm^3). It is therefore possible that the complications during the second sampling campaign subsequently discussed (including the second and third layers of S2), led to an unrepresentative sampling of the second layer. This hypothesis is supported by the low R^2 value (0,69).

AWC is shown in Table 4. The sandy-loam soil (S2) has an lower AWC and a higher water content at the wilting point than the clay soil (S1). As a clay soil should have a higher residual water content, this could be due to the formation of aggregates in S2 holding more water under high tensions. The inter-aggregated pores also increase macroporosity (Jacinto et al., 2012), it may illustrate the highest water content at saturation in S2 compared to S1 observed in Figure 10a(2). The AWC difference between S1 and S2 is due to the microporosity (macroporisty doesn't impact AWC), as shown in Figure 9a(B) and 10a(B), microporosity distribution is larger in S1 than S2. This measure is corroborated by the high rate of silt and clay in S1 compared to S2 (Table 1).
In other words, S2 could have two distinct porosities due to the formation of aggregates, a microporosity impacting water content at the wilting point and a macroporosity impacting water content at saturation but not AWC. S1 has a less developed macroporosity, but a better AWC due to its texture containing a higher content of silt and clay than S2.

It would be interesting to observe the porosity by tomography for these two soil types, in order to confront these hypotheses.

Table 4: Available water capacity based on water retention curves for Prateah Lang (S1) and Prey Khmer (S2) soil types

	Field Capcity $[cm^3/cm^3]$		**Wilting point** $[cm^3/cm^3]$		**AWC** $[cm^3/cm^3]$	
Horizon	**S1**	**S2**	**S1**	**S2**	**S1**	**S2**
1	0,22	0,21	0,13	0,16	0,09	0,05
2	0,22	0,23	0,13	0,17	0,09	0,06
3	0,27	0,22	0,20	0,19	0,07	0,03
1+4t/ha	0,26	0,16	0,21	0,11	0,05	0,05
1+6t/ha	0,24	0,16	0,19	0,14	0,05	0,02

ii Biochar application

Biochar application in clay soil (S1) tends to increase α and decrease n shape parameters. The opposite effect appears in the sandy-loam soil (S2) (Appendix E). These variations imply that the value of the slope decreases for S1 (increases for S2) for the WRC, increasing

(decreasing) the range of pressure over which there is a variation of water content (Figure 9b(1) and 10b(1)).

In the clay soil (S1), biochar enhanced the macroporosity (Figure 9b(2)). This change in the macroporosity impacts the water content in the range of low tension values (i.e. near the saturation). There is also a change in microporosity, like the residual water content confirms (0,12 to 0,15 and $0{,}16 cm^3/cm^3$ for $4t/ha$ and $6t/ha$). Castellini et al. (2015) also observed an increase in porosity (microporosity) and structure (macroporosity) in clay soil. However, this article also summarizes several studies showing a decrease in microporosity.

With biochar application, the macroporosity of the sandy-loam soil (S2) does decrease, as shown by the small fluctuation in volumetric water content at saturation. While the microporosity seems to be increased by the modification of water content dynamics under high tension (pF>1,78) (Figure 10b(1)). These results are not in agreement with the literature, indicating an increase in total porosity with a sandy-loam soil texture (Githinji, 2014; Abel et al., 2013). However, as mentioned above, there may be aggregate formation in this horizon, and the homogenization of biochar in the first layer by plowing may have degraded these inter-aggregates interaction leading to a soil with less structure (macroporosity). In consequence, the frequency of microporosity increased (Figure 10b(2)).

The conclusion for the application of biochar based on water retention and porosity curve is that for S1, the water content response (i.e. the tension range over a change in water content appear) is improved but not the AWC by increasing the total porosity. Water content response and AWC of S2 are diminished by a possible modification of soil structure (i.e. macroporosity).

Nevertheless, the second sampling campaign can be questioned and thus the divergent results of the S2 biochar application and the second S2 horizon can be as well. Firstly, some columns revealed pockets of air inside, which could indicate a disassociation of the soil inside the column during sampling and therefore a modification of the structure. Secondly, due to difficulties during the second campaign, the three replicates for pressure plate measurements were taken from the same column, questionning the random, simple and independent sampling. Thus, the samples could reflect local heterogeneities.

Finally, the temporal arrangement of the experiment made it impossible to measure the impact of biochar on the saturated conductivity. It would have been interesting to measure it in order to compare these results with the literature, showing positive but also null results on conductivity by biochar (Castellini et al., 2015; Lim et al., 2016; Wang et al., 2021). In addition, Lu et al. (2019) underlines the alteration of porosity by the application of fertilizer, a future experiment should also take this into consideration.

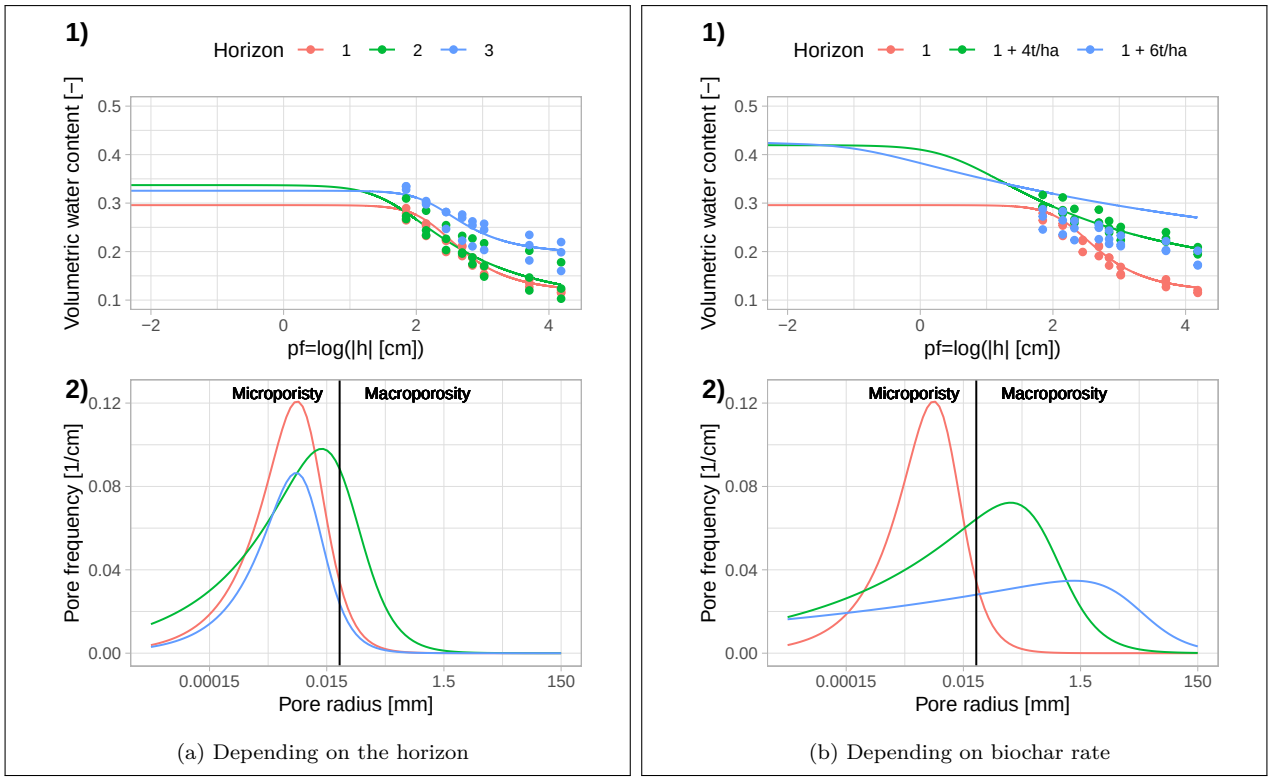

(a) Depending on the horizon

(b) Depending on biochar rate

Figure 9: Prateah Lang (S1) water retention (A) and porosity (B) curves of the soil horizons and biochar application

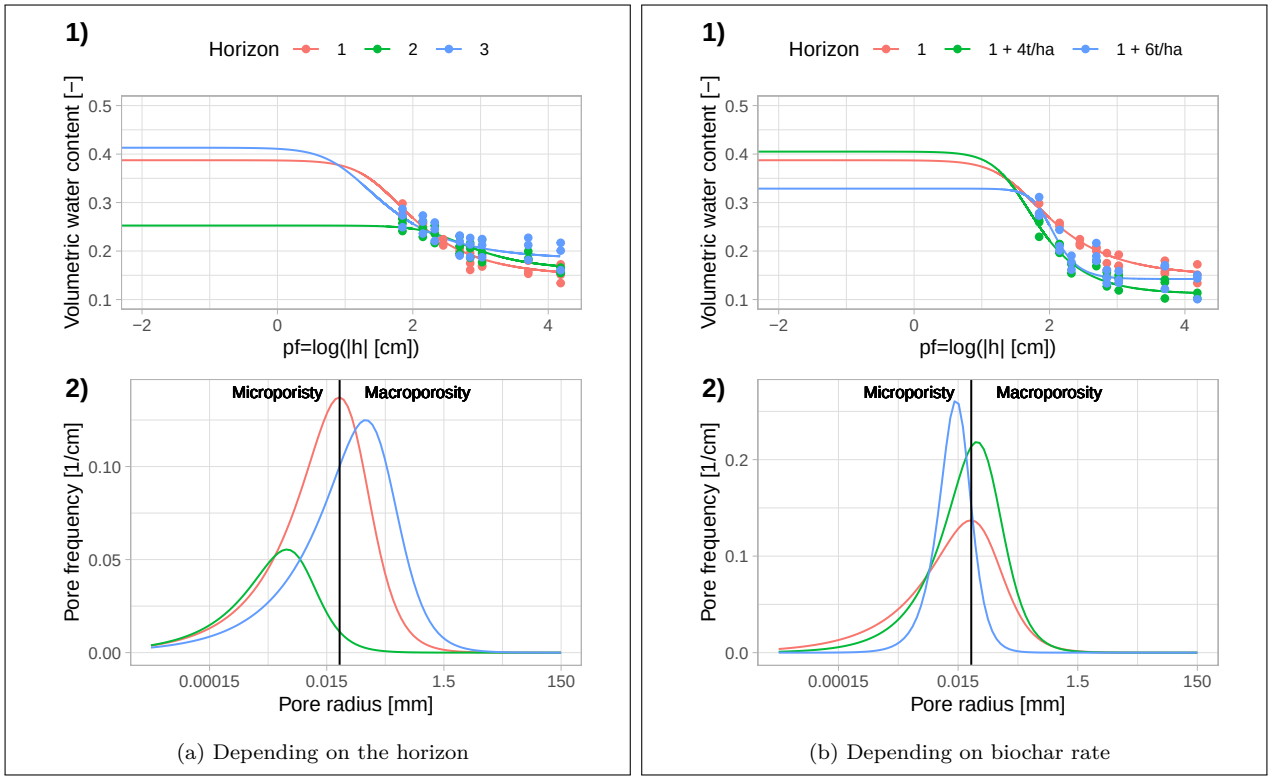

(a) Depending on the horizon

(b) Depending on biochar rate

Figure 10: Prey Khmer (S2) water retention (A) and porosity (B) curves of the soil horizons and biochar application

2 Experimentation

i Root growth and plant height

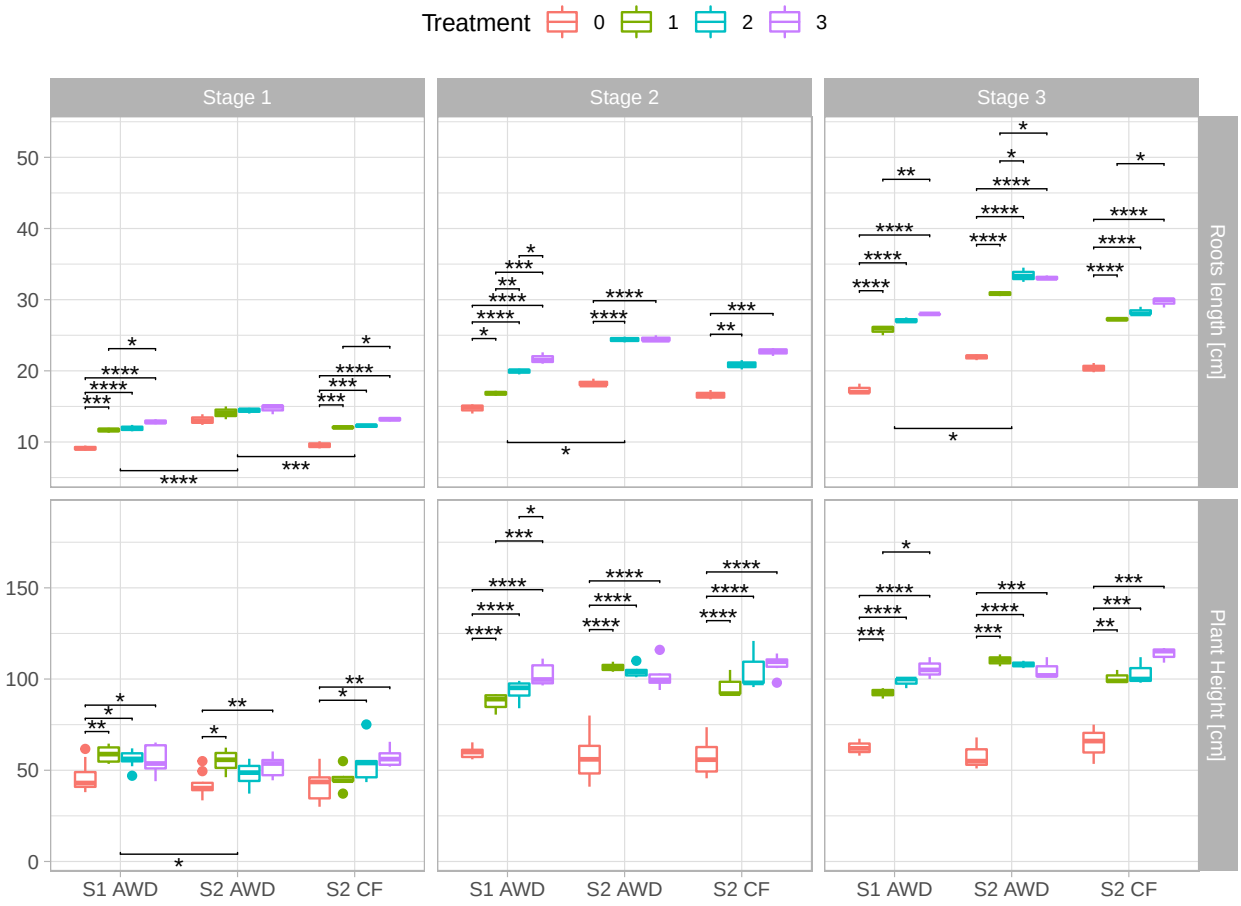

Figure 11: Average root length and plant height comparison. Depending on stages (1: tillering 49 days; 2: boosting 79 days; 3: flowering 89 days) and treatments (0 : no intrants; 1 : SRF; 2 : SRF+4t/ha of biochar; 3 SRF+6t/ha of biochar) for the two soil types (S1 and S2) and the two water management practices (CF and AWD)

Root system

Average root length is significantly different according to soil types and water management practices at stage one and according to soil types only at the other two stages (Figure 11). At the first stage, roots grow deeper in a sandy-loam soil and with alternate water management practices. The same tendency is observed at second and third stages as shown in Table 5, but the difference is not statistically significant.

Although there are conflicting results regarding the relationship between root growth and water accessibility in the literature (Cairns et al., 2011), several studies attest that water stress positively impacts roots grow, as observed between S2-CF and S2-AWD (Mambani and Lal, 1983; Yang et al., 2004).

The difference between the two soil types is explained by different factors. Firstly, for S2, the root penetration stress is lower due to coarser texture and lower bulk density (Table 1) (Cairns et al., 2011)). Secondly, AWD creates a matrix attraction in the root zone by decreasing the matrix water content. Therefore, the higher amount of clay and silt content in S1, increase the penetration constraint during drying conditions (Cairns et al., 2011).

Due to a lack of repetition (n=1), the treatment one is not taken into consideration for S2-AWD and S2-CF (Figure 11).

Treatments with fertilizer are significantly different at every stage and experiment condition, except at the first stage of S2-AWD (Figure 11). Therefore, SRF has a positive effect on root growth (Yang et al., 2021).

As shown in Figure 11, $6t/ha$ of biochar promotes root growth for S1-AWD at every growth stage, S2-CF at stage one and three and S2-AWD at stage three (missing comparison for S2-AWD and S2-CF at stage two). Biochar application rates enhances root growth proportionally for S1-AWD and S2-CF. However, the difference in root growth with $4t/ha$ of biochar is not great enough to lead to a statistical difference with treatment one. For S2-AWD there is no difference regarding to biochar quantities.

This root growth promotion is due to biochar's side-effects such as increased soil pH (i.e. increasing nutrients' availability), CEC, EC, and microbial interaction (Muhammad et al., 2018). Therefore, there is a promotion of nutrient use efficiency with biochar application even in water stress conditions. The efficiency rate is $6t/ha$.

In addition, increasing the number of repetitions for root length measurements would allow stronger statistical analysis and a possible difference in average appearance.

Plant height

Except between the two soil types at the first stage of growth, there is no statistical difference in plant height for different soil types and water management practices. Moreover, there is no observable trend in the average plant height (Table 5).

As presented in the soil properties analysis in Table 1, S1 possesses better fertility indicators than S2, except for the pH (Acidic pH, reducing plant nutrients availability). These differences may impact the first stage of development, promoting better conditions for plant growth at the beginning. At the two other stages, intrants, which have had time to integrate in the soil, may compensate the initial difference of fertility.

SRF has an effect on plant height (Yang et al., 2021). This effect is statistically proven at stage two and three and for S1-AWD at stage one (Figure 11). As previously stated, the

fertility of S1 improves fertilizer stabilization, resulting in a statistically significant difference at the first stage.

At stages two and three, S1-AWD is positively impacted by biochar presence as well as S2-CF, while S2-AWD shows a negative impact of biochar on plant height. However, except for $6t/ha$ of S1-AWD, there is no statistical difference. These trends are not observed at stage one because the biochar has not yet stabilized in the soil. These observations will be discussed in further detail below.

Table 5: Average root length and plant height depending on stages (1 :tillering 49 days; 2: boosting 79 days; 3: flowering 89 days)

	Root length [cm]			**Plant height** [cm]		
Stage	**1**	**2**	**3**	**1**	**2**	**3**
S1-AWD	11,3	18,4	24,5	54,0	85,7	89,7
S2-AWD	14,1	22,2	29,7	48,4	91,4	96,0
S2-CF	11,7	19,9	26,3	49,7	90,8	101,5

Comparison of the two indicators

Compared to root growth, the difference between the experimental conditions is less significant for height. Due to direct application in the vadoze zone, biochar has a stronger impact on root length than it has plant development (Sohi et al., 2010).

The two applications of SRF improved the height and root length of the plant during the experiment. This result is supported by Yang et al. (2021), which concludes that SRF owns benefits over conventional fertilizer (regular urea) in terms of productivity and economy. SRF is therefore advantageous for rice productivity.

Impact of biochar application is less significant compared to SRF. S1-AWD and S2-CF show greater growth with biochar, this is less marked for S2-AWD. However, as shown in section III.1, the water response range depending on tension is diminished for S2 with biochar application. In consequence, S2-AWD water stress is amplified by biochar presence. It has negative effect on water response for S2 and positive side effects on the vadoze zone (pH stability, increase of CEC, EC, and microbial interaction) resulting in an increase of root development but a decrease of plant height.

It would have been interesting to compare grain yields, since this is the economical indicator defining the durability of an agricultural practice. In addition, using root mass instead of length would have provided a better comparison, representing the growth of the root system. Moreover, since biochar is always applied in combination with SRF in this experiment, it is difficult to apply a covariance test to assess whether biochar alone would have had an influence.

ii Percolation water

Figure 12 represents percolative cumulated water depending on stages, soil types, water management practices and treatments. Because there are fewer columns between each stage, it was necessary to divide the statistical analysis.

The statistical conditions are adhered to, except for the equality of the variance at the first stage. Indeed, at the beginning of the experiment, the clay texture led to preferential flows at the edge of some columns, resulting in variability in the percolation volume for S1. Afterwards, the soil was restructured in the column, decreasing these preferential flows.

Clay soil (S1) has a lower percolation volume than sandy-loam soil (S2). The AWC of S1 is greater compared to S2 (Table 4). This soil can contain more water, reducing the amount of gravitational water. In addition, the lower conductivity of clay soil allows water to remain longer in the soil, increasing the probability of evaporation and transpiration.

Appendix F represents variance analysis depending on treatments, soil types, water management practices and days. There are five significant differences of which two (S2-CF day 21 and S2-AWD day 35) don't respect variance equality. Those differences are erratic, which lead to consider that treatments have no impact on percolation.

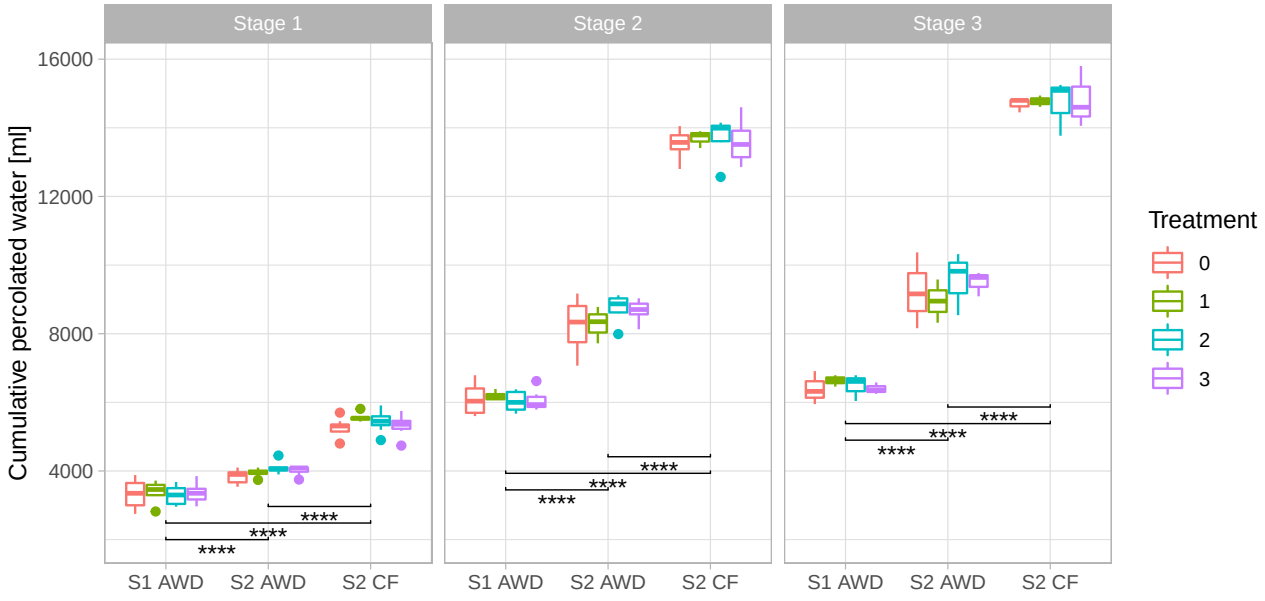

Figure 12: Average cumulative percolated water. Depending on stages (1: tillering 49 days; 2: boosting 79 days; 3: flowering 89 days) and treatments (0 : no intrants; 1 : SRF; 2 : SRF+4t/ha of biochar; 3 SRF+6t/ha of biochar) for the two soil types (S1 and S2) and the two water management practices (CF and AWD)

Conductivity and water content sensors or a balance to continually collect the mass of percolated water should be set up for a future experiment to highlight the difference of water dynamics depending on treatments. A discontinuous measure in percolation does not effectively represent local changes in a soil column affected by many layers in a continual temporal dimension.

iii Nutrient transport

Figure 13 shows the nutrient concentration in the water flow at the first node (h=-15cm). However, the measure of the quantity of leached nutrient is in progress.

For the various treatments, NH_4^+ and PO_4^{3+} ions' leaching at h=-15cm is higher for S2-AWD than for S1-AWD. Because of its finer texture, which increases specific surface area, S1 has a higher CEC and EC than S2 (Table 1). As a result, more ions are adsorbed in S1, which reduces the nutrient concentration in the percolated water. The difference for NO_3^- is less pronounced. Anionic exclusion appears for NO_3^- on soil materials and organic matter which are negatively charged (Allred et al., 2007). Moreover, the flow rate is slower for S1, increasing the exchange time between the soil solution and the percolating water.

A greater concentration of nutrients is shown for the S2-AWD regime than for the S2-CF regime, with the exception during the first 25 days of NH_4^+ treatments two and three and for PO_4^{3+} treatment zero. Two complementary phenomena may explain this disparity. Firstly, nitrification occurs in anaerobic conditions, transforming more NH_4^+ into NO_3^- in CF conditions. Secondly, since CF irrigation causes the SRF to dissolve more frequently, the concentration of nutrients is more diluted in the percolated water. However, Tan et al. (2015) indicates that nitrogen is leached more due to the changes between anaerobic and aerobic conditions of AWD, leading to an increase in N losses. The nutrients leaching quantity measurement in progress may corroborate these hypotheses.

No explanation could be found for the phenomena that lead to a higher NH_4^+ concentration for the treatments two and three of S2-CF during the first 25 days.

Overall it appears that the curves with the biochar treatments undergo less leaching. As mentioned above, biochar application increases pH, CEC, EC and stimulates microbial activity. Therefore, the adsorption by soil's particles and absorption by plants and microbiota are enhancing.

The installation of suction cups would have made it possible to see the difference in concentration between the matrix water and the gravity water, allowing a deeper understanding of the different results mentioned above. In addition, a soil containing century charcoal shows modifications on hydraulic properties (Zanutel et al., 2022), and in solute balance by increasing the CEC (Hardy et al., 2017). Consequently, as biochar is very persistent and can be prepared differently from several materials (Sohi et al., 2010), a multiple year study should be managed

to emphazise its effects on the long term on Prey Khmer and Prateah Lang soils and examine the effects of different biochar species.

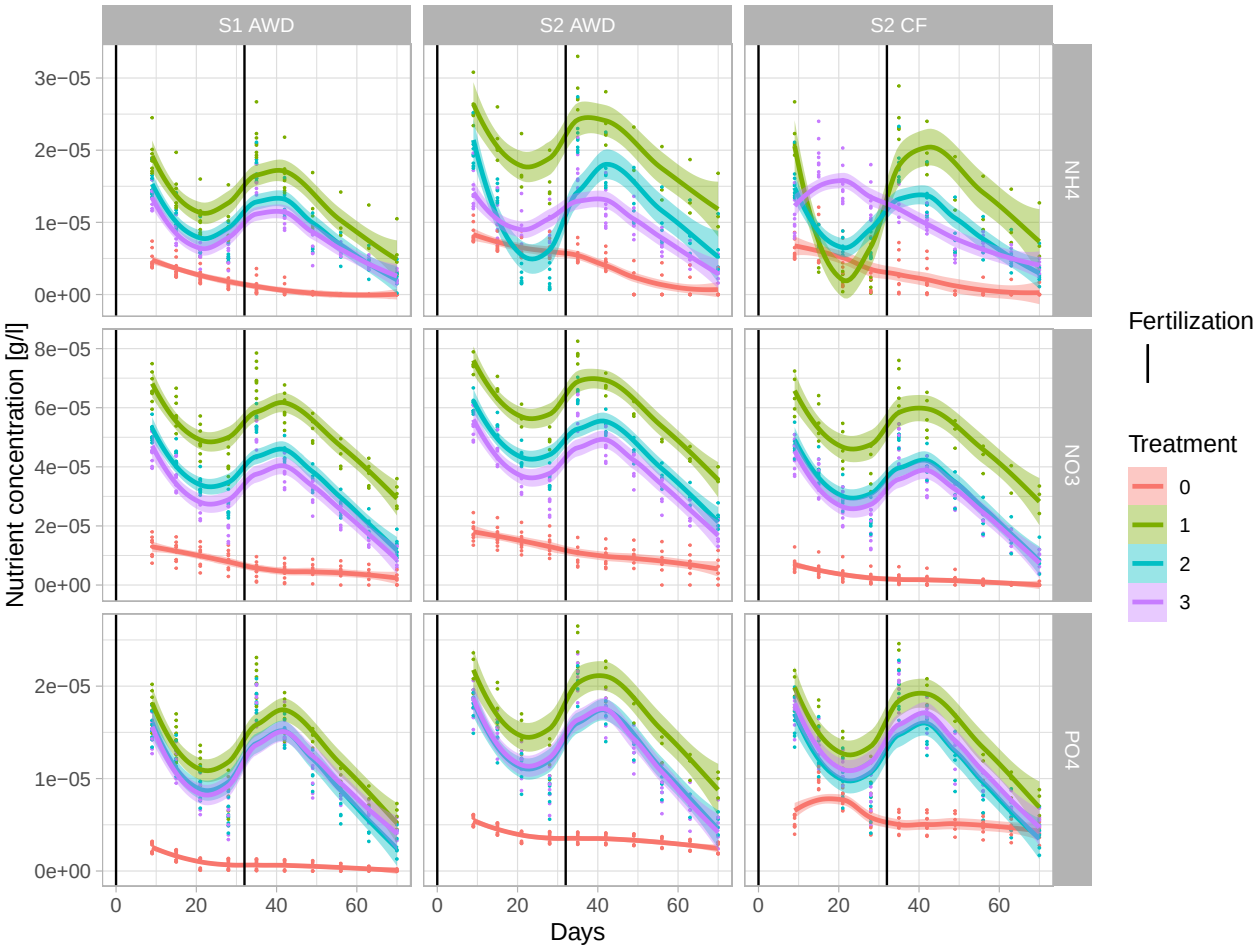

Figure 13: Evolution of the nutrient concentration in the water flow from the first observation valve (h=-15cm) with two applications of SRF (days 0 and 32)

3 Model

i Water balance

As discussed in section III.ii, percolation shows no statistical difference between treatments (Figure 12). In order to increase statistical stability, only three sets of data (one for every soil and every water management practices) were created for water balance by gathering measurements of the different treatments. In addition, an attempt was realized to measure the conductivity modification caused by biochar. Indeed, because the application had changed the water response (i.e. water content variation over tension range) of the soils, an inverse solution based on percolation could be used to approximate K_s. Table 6 shows the value of the modified parameters and quality model statistical indicator NSE. Models with only one NSE value were not calibrated.

The statistical quality of S1-AWD models are very good ($\simeq$ 0,91). However, a different approach was used owing to HYDRUS-1D's non-convergence of K_s estimation of horizons with biochar : shape parameters (α and n) and K_s were fitted rather than only K_s and the initial values were identical to the first layer without biochar application. The calibration has no impact on α (0,01cm^{-1}) and increases the parameter n for 6t/ha rate only (Table 7). In comparison to the first layer without intrants, the K_s values for the two biochar rate models (2,17 for 4t/ha and 1,7 for 6t/ha) are greater than the measurement (0,58cm/day) but lower than the calibration (4,6cm/day).

S2-AWD models show very good statistical indicators of modeling. The model fitted with 4t/ha biochar parameters shows better representation of the measured percolation than the 6t/ha (Table 6). The fitted K_s is equal to 2,10, 2,22 and 2,49cm/day for the model with initial hydraulic parameters of 4t/ha, 6t/ha of biochar and without, respectively.

Models of S2-CF represent the field observations with unsatisfactory results. Consequently, the fitted parameters (220, 7 and 96, 4cm/day) are considerably higher than the initial value (19,44 cm/day).

NSE for every model of S1-AWD is very good. However, the inability to calibrate only K_s of the two biochar rate values suggests that there could be an issue with the measured values of n and $alpha$ of 4t/ha and 6t/ha. Indeed, the code failed to compile due to inverse solution input data before the 21 first days. This indicates that the flow model estimated with n and α initial parameters differed significantly from the first measurements of the experiment. However, the hydraulic parameter measurement was made after 49 days, when the biochar had time to be integrated into the soil. It may be possible that the hydraulic parameters of the soil changed during the experiment, leading to different flow dynamics afterwards. In other words, the inverse solution is not able to compute a solution for the beginning of the experiment with initial values representing a later stage of the experiment. Another possibility that there is a

problem with the measurements of the hydraulic parameters as mentioned above (Section III.i).

The inverse model suggested a greater conductivity at saturation than the direct measurement for the first layer without intrants. This is in accordance with the difference between measurement and literature mentioned in section III.i. As concluded in Castellini et al. (2015), biochar application seems to decrease the conductivity at saturation. However, the few percolated measurements do not allow to accurately represent the flow dynamics. These results are therefore only assumptions.

Figure 14a represents the percolation resulting from the three different models of S2-AWD. The difference between $6t/ha$ and 0 or $4t/ha$ of biochar rate is due to the total evaporation rate ($\simeq$-15cm for $4t/ha$ or $0t/ha$ and -30cm for $6t/ha$). Biochar application, as mentioned in section III.1, increases the microporosity in the first layer. In this situation, a higher amount of water may ascend through capillarity under lower tension, to be evaporated. This may be detected by the cumulative evaporation rate (Figure 14a), and also by the tension at the surface reaching the wilting point less often (Figure 14b).
This observation implies that the positive effects of microporosity increased for AWD water management practice, allowing the soil to avoid strong local hydraulic stress.

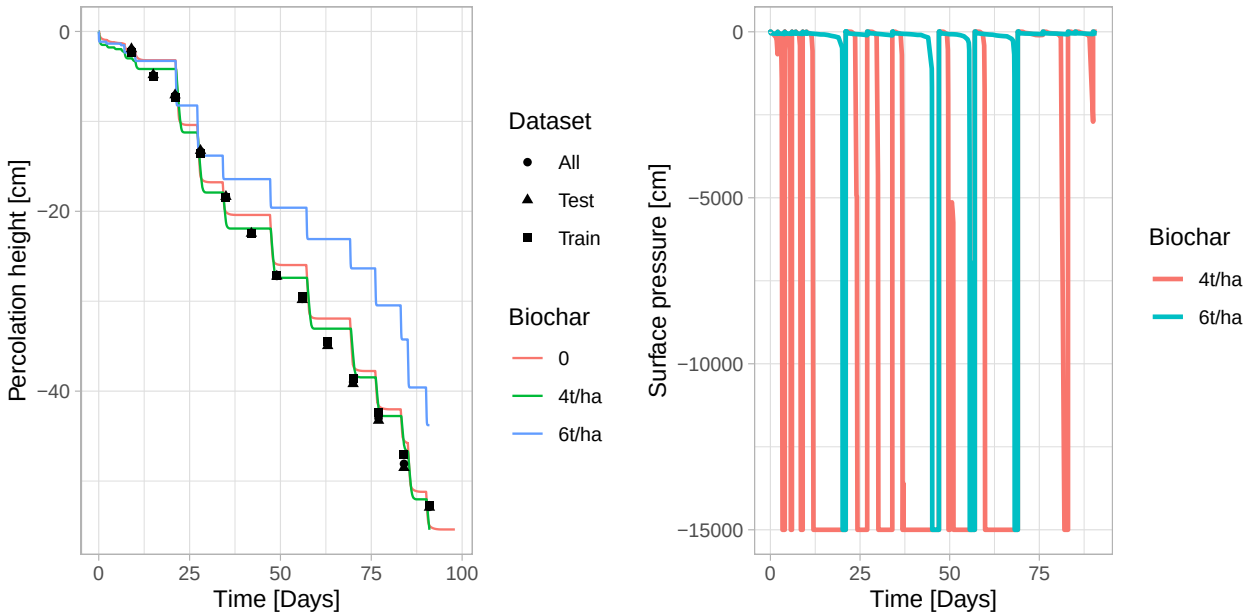

(a) (b)

Figure 14: Evolution of percolation height (a) and surface pressure (b) of the S2-AWD models

In comparison to similar results concerning conductivity at saturation and the biochar application, the same assumptions described for S1-AWD may be applied for S2-AWD.

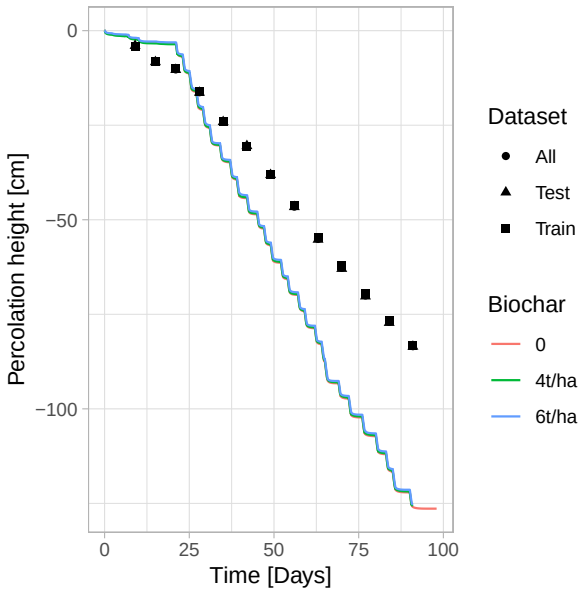

Figure 15: Evolution of percolation height of S2-CF models

For S2-CF, there is a significant difference between the total percolation measurement ($83cm$) and the input water ($164cm$) leading to an inaccurate model as shown in Figure 15. To complete the water balance between irrigation and percolation, the columns of S2-CF should evaporate and transpire over half of the water input. However, the sum of the ET_0 is equal to 39,08 cm and does not reach this difference. Consequently, there is an underestimation of percolated water or an overestimation of irrigated water. Recent information reveals that errors appeared in the irrigation input dataset for S2-CF. This one should be reviewed.

The results discussed above for model accuracy of S1-AWD and S2-AWD without calibration, conclude that HYDRUS-1D succeeded in modeling the experiment. The percolation rate or irrigation should be reviewed for S2-CF. The models of the inverse solution might be questioned. Firstly, the observations of percolation rate do not accurately reflect the flow dynamics, as discussed in section III.ii. Secondly, it might be inaccurate, because the experiment did not take into account the evolution of the soil hydraulic parameters through the stabilization of the biochar. Finally, the inverse solution data used for each model of soil and water management practices are identical. As a result, the estimated changes in conductivity are dependent on the various initial hydraulic parameters that were measured.

Table 6: Statistical analysis and models results of water balance

	Biochar	α	n	Ks	**NSE**		
		$[cm^{-1}]$	[-]	$[cm/day]$	Test	Train	
S1-AWD	0	-	-	-	0,90		Very good
	0	-	-	4,6	0,93	0,93	Very good
	$4t/ha$	0,01	1,68	2,17	0,92	0,91	Very good
	$6t/ha$	0,01	2,39	1,70	0,92	0,92	Very good
S2-AWD	0	-	-	-	0,98		Very good
	0	-	-	2,49	0,98	0,98	Very good
	$4t/ha$	-	-	2,10	0,98	0,99	Very good
	$6t/ha$	-	-	2,22	0,71	0,73	Very good
S2-CF	0	-	-	-	0,12		Unsatisfactory
	$4t/ha$	-	-	220,7	0,15	0,11	Unsatisfactory
	$6t/ha$	-	-	96,4	0,17	0,13	Unsatisfactory

ii Nutrient balance

Some modalities of the experiment were impossible to be represented in HYDRUS-1D. As mentioned in Šimůnek et al. (2012), the fact that the Marquardt-Levenberg method only looks for a local minimum of the objective function is a considerable disadvantage of the method. When there are several soil horizons or solutes, unclear initial conditions, this will be a difficulty for various field-scale situations. In this case, the objective function can have several local minima complicating the computation. Due to that, a simplification in the number of horizons was conducted (Table 9) on almost every model of S2-AWD to perform the computation of nutrient transport. Indeed, the first sampling depth was located at h=-15cm in the second horizon of S2-AWD, therefore the model considered the first layer to extend at -15cm instead of -10cm.

In addition, as discussed in section III.i the number of percolation measurements was insufficient to compute a precise water regime reflecting water dynamics. For this reason, the nutrient models with the current number of concentration measurements were impossible to compute. Therefore, to compute nutrient transport, a continuous flow was simulated.

After a sensitivity study of model performances, the SRF degradation was determined to be a first-order degradation over 10 days.

A one-site sorption model was selected to represent potential preferential fluxes and kinetically controlled sorption. An instant equilibrium model did not allow accurate modeling of the experiment, and a model with more parameters is impossible due to the number of nutrient measurements.

The modeling results for nutrient transport simulated across the top 15cm of the soil profile are summarized in Tables 7 and 9. NO_3^- and NH_4^+ are simulated in the same model.

The marked difference between test and train in these tables attests the variation in dataset. The number of replications ranging from nine to three depending on the stage, should be increased.

Phosphorous transport

Except for treatment one of S1-AWD and treatment zero of S2-AWD and S2-CF, the rest of the models are very good (Table 7). Apart from S2-CF's third treatment, every model overestimates flux concentration.

No SRF was applied in treatment zero, therefore the measurement was only based on nutrient soil stocks (Table 1). An underestimation of S2-AWD stock lead to an impossible computation for S2-AWD and a negative Pbiais for S1-CF (Table 7).

Table 7: Statistical analysis of PO_4^{3+} models

	Treatment	**Simplification**	**Pbiais** [%]		
			Train	Test	
S1-AWD	0	-	-24,9	-32,6	Very Good - Good
	1	-	-49,6	-47	Satisfactory
	2	-	-12	-2,9	Very good
	3	-	0,5	-0,7	Very good
S2-AWD	0	-	-	-	-
	1	No	-11,9	-12,8	Very good
	2	No	-0,3	-4,8	Very good
	3	Yes	-23,9	-24,8	Very good
S2-CF	0	Yes	-48,7	-55,8	Satisfactory
	1	Yes	-3,4	-9	Very good
	2	Yes	-25	-22,5	Very good
	3	Yes	6,1	12	Very good

Calibrated variables are shown in Table 8. It is difficult to extract a pattern between treatments.

The consideration of two horizons was possible for three out of eight models. However, the parameters differ significantly between the two considered horizons (Table 8). This demonstrates that it is more accurate to consider a unique horizon when there is two horizons influencing one measurement site.

Longitudinal dispersivity (D_l) is influenced by pore size distribution, heterogeneity and preferential soil flows. Biochar application should increase this parameter as observed in S2-CF but not in S1-AWD.

The adsorption coefficient (K_d) is the fraction of solute retained by soil particles. The range of K_d values (0,64-26,146cm^3/g) is low compared to the literature (19-185cm^3/g) (Filipović et al., 2020). This might be the result of inadequate SRF degradation representation and the continual irrigation assumption. The measured concentrations are therefore higher for a larger modelled water flux, simulating lower adsorption.

The uncertain discussion above is mainly due to the lack of measurement data, preventing the description of leaching dynamics through the soil and a comparison of leached nutrients amount. It will be possible to identify the kinetics of nutrient transport more clearly after obtaining the other measurements.

Table 8: Transport and transformation parameters of PO_4^{3+} models

	Treatment	Transport parameters				Transformation parameters	
		$D_{L,1}$ $[cm]$	$K_{d,1}$ $[cm^3/g]$	$D_{L,2}$ $[cm]$	$K_{d,2}$ $[cm^3/g]$	α_1 $[day^{-1}]$	α_2 $[day^{-1}]$
S1-AWD	0	0,041	8,357	0,000	0,000	0,000	-
	1	7,716	2,342	-	-	0,028	-
	2	0,425	5,407	-	-	0,017	-
	3	0,219	4,260	-	-	0,023	-
S2-AWD	-	-	-	-	-	-	-
	1	4,500	4,179	0,000	11,556	0,119	0,481
	2	6,449	26,146	0,102	44,542	0,006	0,149
	3	4,500	0,640	-	-	0,094	-
S2-CF	0	4,289	0,866	0,024	52,932	0,136	0,284
	1	0,572	3,915	-	-	0,138	-
	2	4,500	5,184	-	-	0,134	-
	3	4,500	0,640	-	-	0,094	-

Nitrogen transport

The initial soil concentration of nitrogen was an approximation. Indeed, to perform nitrogen concentration measurement, the Kjeldahl method with mineralization of nitrogen was performed. Due to the inability to differentiate chemical solutes and the importance of NO_3^- leaching, N concentration measurements were assumed to be NH_4^+ only.

As previously stated, Marquardt-Levenberg is not optimal to represent the transport of several solutes through multiple horizons. As a result, firstly, the simplification of horizons on S2 was applied to every model. Secondly, NH_4^+ is underrepresented in comparison to NO_3^- (Table 9). It should be possible to prevent this misinterpretation by raising the statistical weight of NH_4^+.

Table 9 summarizes models' statistical analysis. Only the S1-AWD treatment zero model has a poor statistical indicator for both chemical species investigated. The other models have a good to very good indicator for at least one of the two species. Incorrect modeling of S1-AWD treatment zero might result in an underestimation of N stock.

Table 9: Statistical analysis of NO_3^- and NH_4^+ models

	Treatment	**Nutrient**	**Simplification**	**Pbiais** [%]		
				Train	Test	
S1-AWD	0	NH_4^+	-	209,9	171,0	Unsatisfactory
	0	NO_3^-	-	51,6	30,4	Satisfactory-Good
	1	NH_4^+	-	44,6	71,8	Good-Unsatisfcatory
	1	NO_3^-	-	-1,9	-3,4	Very good
	2	NH_4^+	-	54,3	73,1	Very good
	2	NO_3^-	-	-3,6	6,2	Very good
	3	NH_4^+	-	44,3	45,7	Satisfactory
	3	NO_3^-	-	-5	-0,5	Very good
S2-AWD	0	NH_4^+	Yes	-8,2	-26,8	Very good-Good
	0	NO_3^-	Yes	3,1	40	Very good-Good
	1	NH_4^+	Yes	1,2	6,7	Very good
	1	NO_3^-	Yes	-1,4	-6,6	Very good
	2	NH_4^+	Yes	81	111	Unsatisfactory
	2	NO_3^-	Yes	-31,7	-26,7	Good
	3	NH_4^+	Yes	10,8	11	Very good
	3	NO_3^-	Yes	-0,3	4,7	Very good
S2-CF	0	NH_4^+	Yes	-29,3	-28,5	Good
	0	NO_3^-	Yes	177,4	203,5	Unsatisfactory
	1	NH_4^+	Yes	116,6	117,2	Unsatisfactory
	1	NO_3^-	Yes	-1,1	-1,5	Very good
	2	NH_4^+	Yes	-11,7	-4,1	Very good
	2	NO_3^-	Yes	-2,8	16	Very good
	3	NH_4^+	Yes	9	5,2	Very good
	3	NO_3^-	Yes	-15,5	-19	Very good

The parameters of Table 10 indicate that the models consider rates of nitrification ($\mu'_{w,1}$), denitrification ($\mu_{w,2}$) and volatilization ($\mu_{w,1}$) to be higher than immobilization ($\gamma_{s,1}$). Compared to a similar model approach study using urea fertilizer on a sandy-loam without hydraulic stress (Shekhar et al., 2021a), the volatilization rate ($0{,}07day^{-1}$) and adsorption ($3{,}5cm^3/day$) are higher, the nitrification ($0{,}13day^{-1}$) and denitrification ($0{,}1day^{-1}$) are lower, immobilization is equivalent ($0{,}0018day^{-1}$). However, studies show that SRF could reduce nitrogen volatilization and losses (Chen et al., 2021; Jadon et al., 2018; Dong et al., 2016), and AWD should increase nitrification and denitrification rate (Tan et al., 2015), which does not correspond to the calibrated parameters. As for PO_4^{3+}, the representation of SRF degradation combined with the flow assumption may be questioned.

Table 10: Transport and transformation parameters of NO_3^- and NH_4^+ models

	Treatment	N Transport parameters		N Transformation parameters				
		$D_{L,1}$ $[cm]$	K_d $[cm^3/g]$	$\mu_{w,1}$ $[day^{-1}]$	$\mu'_{w,1}$ $[day^{-1}]$	$\gamma_{s,1}$ $[day^{-1}]$	α_1 $[day^{-1}]$	$\mu_{w,2}$ $[\mu day^{-1}]$
S1-AWD	0	0,001	8,756	0,291	0,038	0,001	7,14E-06	0,050
	1	15,086	78,552	0,000	0,060	0,000	2,87E-04	0,000
	2	17,687	21,217	0,106	0,035	0,000	2,95E-04	0,021
	3	17,955	19,768	0,148	0,024	0,000	2,64E-04	0,027
S2-AWD	0	0,001	7,097	0,158	0,059	0,001	2,88E-06	0,030
	1	37,484	5,235	0,103	0,060	0,000	8,63E-04	0,009
	2	0,036	6,064	0,031	0,060	0,001	1,21E-05	0,043
	3	0,158	2,810	0,131	0,060	0,001	1,08E-05	0,016
S2-CF	0	1,542	8,459	0,157	0,039	0,001	1,69E-09	0,028
	1	34,798	4,043	0,107	0,037	0,000	8,39E-05	0,010
	2	42,813	10,723	0,169	0,060	0,000	3,65E-04	0,027
	3	0,000	7,403	0,086	0,060	0,001	1,05E-05	0,028

In conclusion, it was possible to develop models with appropriate statistical indicators despite actual parameter values by ignoring the irrigation dynamics and multiple horizons for S2. Due to the limited number of nutrient concentrations, it was impossible to fit models without these assumptions.

The development of these models remains to be done. After receiving the nutrient concentrations at the different sampling points of the column, it will be possible to improve the models following the steps presented in Figure 16. A reliable model considers good statistical indicators and meaningful parameters.

Finally, some points remain to be improved for the modeling part and for a futher experimentation :

- A sensitivity analysis on the effect of the solute degradation time on model performance should be performed again
- The parameter of nitrogen chain immobilization (γ_s) reaction should be removed if similar low values are simulated, to improve inverse solution compilation.
- Statistical weight of NH_4^{3+} and NO_3^- inverse solution data should be modified to improve the simulation of NH_4^+ transport and transformation
- Water dynamics should be measured by another method

Finally, as McCullagh (2019) mentioned, "all models are wrong; some, though, are more useful than others and we should seek those". The modeling method is a simplification based on influential variables that do not accurately interpret reality. The models carried on during this experiment represent water balance and nutrient dynamics for several experimental conditions in a global way. If another experiment should be performed, it will be preferable to reduce the represented variables in order to increase the complementary information provided by the models. Indeed, major challenges in soil modeling across all studies and applications arise from

the fact that the soil environment is heterogeneous, processes take place over a wide range of geographical and temporal dimensions, and one must address uncertainty in both models and data (Vereecken et al., 2016). This complexity, combined with a short-term low-budget project whose aim is not the modeling part, does not allow an accurate interpretation of the results.

IV Contribution

During this mobility, the main goal for the student was to support the experiment designed by the PhD student Chenda LAI and to increment modelling possibility in it. The student achieved to :

- Process soil and laboratory measurements
- Give a support to conduct the experiment
- Develop a project taking into consideration field constraints
- Demonstrate technical ability to adapt to available materials
- Collaborate and take initiatives to accomplish the predetermined objective
- Identify points of consideration and communicate them to parties
- work in a new environment and adapt to the work dynamic

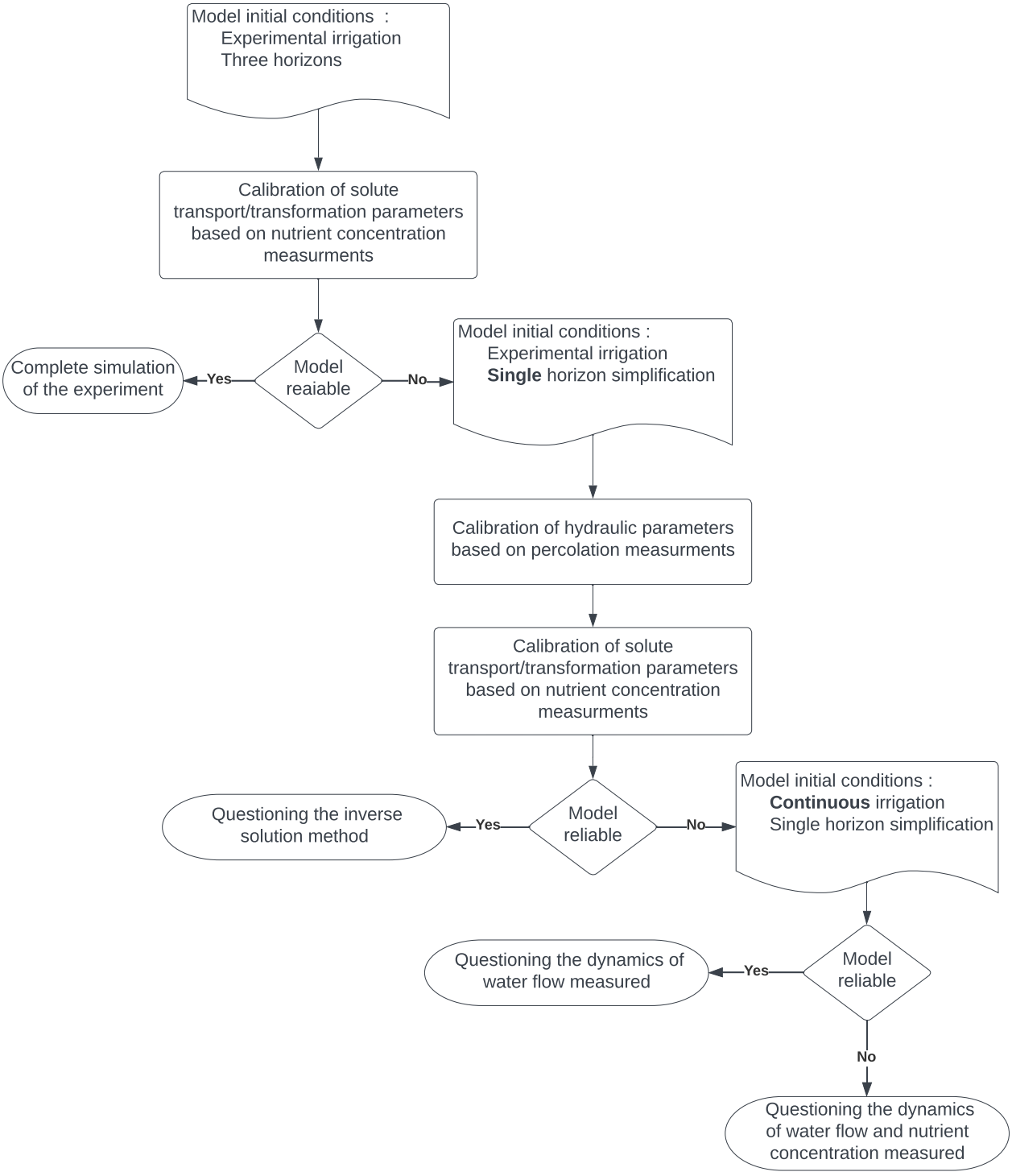

Figure 16: Perspective flowchart resuming the steps of model development

V Conclusion

Developing accessible agricultural sustainable practices becomes an economical and ecological major point in Cambodia. The study project was to create a model to assist an experiment based on biochar, slow-release fertiliser and alternate wetting and drying water management. Two significant agronomic soil types in Cambodia were studied : Prey Khmer, a sandy-loam soil and Prathea Lang, a clay soil.

The experiment started on the 22nd March until 28th of June. Some of the experimental results of the experiment are still being processed, which will provide a complete discussion.

Models of water balance and nutrient transport related to the experimental conditions were created. Afterwards, this will allow a better understanding of the dynamics of water and nutrients, while allowing numerical testing of experimental conditions variation.

The modelling of water balance shows good results for S1-AWD and S2-AWD. For S2-CF, input irrigation data needs to be reviewed.

Nonetheless, the percolated water measurement method was ineffective in highlighting differences in water flow dynamics between biochar and SRF treatments. To prevent this, a continuous measurement of percolation's weight or water content combined with tension sensors for every horizon should be set up for a future experiment.

For nutrient transport and transformation, it was possible to develop models with appropriate statistical indicators despite actual parameter values, by ignoring the dynamics of irrigation and S2's multiple horizons. Due to the limited number of nutrient concentration data, it was not possible to fit models without these assumptions. The development of these models remains to be done when the concentration analysis will be completed.

However, various improvements in the representation of nutrient transport, SRF degradation and measurements are possible. For a future experiment, the complexity of interaction variables in soil combined with a short-term low-budget project, does not permit correct evaluation of the results. It would be preferable to diminish the number of variables of interest and increase the accuracy of measurement over it.

In addition, soil hydraulic properties measurement was performed for the different horizons and the biochar application.

Based on the water retention curves, it was established that biochar affects soil porosity during this experiment. The total porosity of S1 has increased, resulting in a variation in water content over a wider range of tensions. This phenomena and AWC seemed to decrease for S2 by a modification of soil structure.

Parallel to the modelling part, the development of the crops (root and biomass) was monitored. Unfortunately, the yield information is not available.

SRF application enhanced the growth of the root length and plant's height. Biochar improvements are significant on the root system but less on the aerial parts of the rice plant. The modification of the S2 structure with biochar application mentioned above, associated with water stress events, may decrease the plant height. Without taking into account this trend, the optimum growth is achieved when 6t/ha of biochar and SRF are applied. AWD seems to positively impact the root length but not the plant height, leading to a reduction in water input without compromising the plant's development.

Presently, only one concentration measurement depth (-15cm) of percolated water was analysed, not giving the measurement of the quantity of nutrients leached. It seems that S1 adsorbs more ions than S2 ($PO_4^{3+}; NH_4^+;\ NO_3^-$) due to its greater CEC and electrical conductivity. CF shows a decrease of nutrient concentration. However, currently, it is impossible to determine precisely whether the measurements reflect a leaching mitigation or a greater dilution. Overall, it appears that biochar application treatment undergoes less leaching.

Nevertheless, since these measurements represent the water flow concentration, they don't give precise information on the dynamics of nutrients between the soil and the matrix water nor on the amount of nutrients per volume of soil. A deeper analysis based on solutes dynamics through the soil columns, thanks to the concentration analysis in progress, remains to be done.

Finally, a study over the governance of good cropping practices needs to integrate an economical and social aspect. The accessibility to technologies for the agricultural workforce, and the economical benefit including yield and GHG emissions of these practices need to be taken into consideration.

References

Abel, S., Peters, A., Trinks, S., Schonsky, H., Facklam, M., & Wessolek, G. (2013). Impact of biochar and hydrochar addition on water retention and water repellency of sandy soil. *Geoderma*, *202-203*, 183–191. https://doi.org/10.1016/j.geoderma.2013.03.003

Allen, R., Pereira, L., Raes, D., & Smith, M. (1998). FAO irrigation and drainage paper no. 56. *Rome: Food and Agriculture Organization of the United Nations*, *56*, 26–40.

Allred, B. J., Brown, G. O., & Bigham, J. M. (2007). Nitrate mobility under unsaturated flow conditions in four initially dry soils. *Soil Science*, *172*(1), 27–41. https://doi.org/10.1097/01.ss.0000240548.44551.74

Al-Wabel, M. I., Hussain, Q., Usman, A. R., Ahmad, M., Abduljabbar, A., Sallam, A. S., & Ok, Y. S. (2018). Impact of biochar properties on soil conditions and agricultural sustainability: A review. *Land Degradation & Development*, *29*(7), 2124–2161. https://doi.org/10.1002/ldr.2829

Avil Kumar, K., & Rajitha, G. (2019). Alternate wetting and drying (AWD) irrigation - a smart water saving technology for rice : A review. *International Journal of Current Microbiology and Applied Sciences*, *8*, 2561–2571. https://doi.org/10.20546/ijcmas.2019.803.304

Bahmani, O., Sabziparvar, A.-A., Javadi, H., Pak, V., & Nasab, S. (2019). Evaluation of soil nitrate accumulation under different fertigation regimes and simulation by the hydrus-1d model. *Water Conservation Science and Engineering*, *4*. https://doi.org/10.1007/s41101-019-00072-7

Bank, A. D. (2014). *Improving rice production and commercialization in cambodia: Findings from a farm investment climate assessment.* Asian Development Bank.

Bear, J. (1988). *Dynamics of fluids in porous media.* Courier Corporation.

Belmans, C., Wesseling, J. G., & Feddes, R. A. (1983). Simulation model of the water balance of a cropped soil: SWATRE. *Journal of Hydrology*, *63*(3), 271–286. https://doi.org/10.1016/0022-1694(83)90045-8

Cairns, J. E., Impa, S. M., O'Toole, J. C., Jagadish, S. V. K., & Price, A. H. (2011). Influence of the soil physical environment on rice (oryza sativa l.) response to drought stress and its implications for drought research. *Field Crops Research*, *121*(3), 303–310. https://doi.org/10.1016/j.fcr.2011.01.012

Cantrell, R. P. (2004). Challenges and opportunities for rice-based farming in the international year of rice and beyond. *Paddy and Water Environment*, *2*(1), 1–4. https://doi.org/10.1007/s10333-004-0033-8

Carrijo, D. R., Lundy, M. E., & Linquist, B. A. (2017). Rice yields and water use under alternate wetting and drying irrigation: A meta-analysis. *Field Crops Research*, *203*, 173–180. https://doi.org/10.1016/j.fcr.2016.12.002

Castellini, M., Giglio, L., Niedda, M., Palumbo, A. D., & Ventrella, D. (2015). Impact of biochar addition on the physical and hydraulic properties of a clay soil. *Soil and Tillage Research*, *154*, 1–13. https://doi.org/10.1016/j.still.2015.06.016

Chen, L., Liu, X., Hua, Z., Xue, H., Mei, S., Wang, P., & Wang, S. (2021). Comparison of nitrogen loss weight in ammonia volatilization, runoff, and leaching between common and slow-release fertilizer in paddy field. *Water, Air, & Soil Pollution*, *232*(4), 132. https://doi.org/10.1007/s11270-021-05083-6

Chowdary, V. M., Rao, N. H., & Sarma, P. B. S. (2004). A coupled soil water and nitrogen balance model for flooded rice fields in india. *Agriculture, Ecosystems & Environment*, *103*(3), 425–441. https://doi.org/10.1016/j.agee.2003.12.001

Cosslett, T. L., & Cosslett, P. D. (2018). Rice cultivation, production, and consumption in mainland southeast asian countries: Cambodia, laos, thailand, and vietnam. In T. L. Cosslett & P. D. Cosslett (Eds.), *Sustainable development of rice and water resources in mainland southeast asia and mekong river basin* (pp. 29–53). Springer. https://doi.org/10.1007/978-981-10-5613-0_3

CSES. (2020). *Cambodia socio-economic survey reports*. National Institute of Statistics Ministry of Planning.

Das, S. K., & Ghosh, G. K. (2017). Soil hydro-physical environment as influenced by different biochar amendments. *International Journal of Bio-resource and Stress Management*, *8*(5), 668–673. https://doi.org/10.23910/IJBSM/2017.8.5.1841

Dong, Y. J., He, M. R., Wang, Z. L., Chen, W. F., Hou, J., Qiu, X. K., & Zhang, J. W. (2016). Effects of new coated release fertilizer on the growth of maize. *Journal of soil science and plant nutrition*, *16*(3), 637–649. https://doi.org/10.4067/S0718-95162016005000046

FAOSTAT. (2020). Retrieved July 19, 2022, from https://www.fao.org/faostat/en/#data/QCL

Feddes, R. A. (1982). *Simulation of field water use and crop yield*.

Filipović, V., Černe, M., Šimůnek, J., Filipović, L., Romić, M., Ondrašek, G., Bogunović, I., Mustać, I., Krevh, V., Ferenčević, A., Robinson, D., Palčić, I., Pasković, I., Goreta Ban, S., Užila, Z., & Ban, D. (2020). Modeling water flow and phosphorus sorption in a soil amended with sewage sludge and olive pomace as compost or biochar. *Agronomy*, *10*(8), 1163. https://doi.org/10.3390/agronomy10081163

Freiberger, R., Heeren, D., Eisenhauer, D., Mittelstet, A., & Baigorria, G. (2018). Tradeoffs in model performance and effort for long-term phosphorus leaching based on in situ field data. *Biological Systems Engineering: Papers and Publications*.

Giap, G. E., Rudiyanto, & Sulaiman, M. S. (2021). Water infiltration into sand, silt, and clay at field capacity. *Journal of Advanced Research in Fluid Mechanics and Thermal Sciences*, *84*(2), 159–166. https://doi.org/10.37934/arfmts.84.2.159166

Githinji, L. (2014). Effect of biochar application rate on soil physical and hydraulic properties of a sandy loam. *Archives of Agronomy and Soil Science*, *60*(4), 457–470. https://doi.org/10.1080/03650340.2013.821698

GPCC. (2019). *General population census of the kingdom of cambodia 2019*. National Institute of Statistics Ministry of Planning.

Gupta, A., Gupta, M., Srivastava, P. K., Sen, A., & Singh, R. K. (2021). Subsurface nutrient modelling using finite element model under boro rice cropping system. *Environment, Development and Sustainability*, *23*(8), 11837–11858. https://doi.org/10.1007/s10668-020-01144-8

Gupta, H. V., Sorooshian, S., & Yapo, P. O. (1999). Status of automatic calibration for hydrologic models: Comparison with multilevel expert calibration. *Journal of Hydrologic Engineering*, *4*(2), 135–143. https://doi.org/10.1061/(ASCE)1084-0699(1999)4:2(135)

Hardy, B., Cornelis, J.-T., Houben, D., Leifeld, J., Lambert, R., & Dufey, J. E. (2017). Evaluation of the long-term effect of biochar on properties of temperate agricultural soil at pre-industrial charcoal kiln sites in wallonia, belgium. *European Journal of Soil Science*, *68*(1), 80–89. https://doi.org/10.1111/ejss.12395

Hoffman, G. J., & Van Genuchten, M. T. (1983). Soil properties and efficient water use: Water management for salinity control. *Limitations to efficient water use in crop production* (pp. 73–85). John Wiley & Sons, Ltd. https://doi.org/10.2134/1983.limitationstoefficientwateruse.c5

Hopmans, J. W., Šimůnek, J., Romano, N., & Durner, W. (2002). 3.6.2. inverse methods. *Methods of soil analysis* (pp. 963–1008). John Wiley & Sons, Ltd. https://doi.org/10.2136/sssabookser5.4.c40

Ishii, S., Ikeda, S., Minamisawa, K., & Senoo, K. (2011). Nitrogen cycling in rice paddy environments: Past achievements and future challenges. *Microbes and Environments*, *26*(4), 282–292. https://doi.org/10.1264/jsme2.me11293

Jacinto, A., Villar, M., & Ledesma, A. (2012). Influence of water density on the water-retention curve of expansive clays. *Géotechnique*, *62*(8), 657–667. https://doi.org/10.1680/geot.7.00127

Jadon, P., Selladurai, R., Yadav, S. S., Coumar, M. V., Dotaniya, M. L., Singh, A. K., Bhadouriya, J., Kundu, S., Jadon, P., Selladurai, R., Yadav, S. S., Coumar, M. V., Dotaniya, M. L., Singh, A. K., Bhadouriya, J., & Kundu, S. (2018). Volatilization and leaching losses of nitrogen from different coated urea fertilizers. *Journal of soil science and plant nutrition*, *18*(4), 1036–1047. https://doi.org/10.4067/S0718-95162018005002903

Jha, R. K., Sahoo, B., & Panda, R. K. (2017). Modeling the water and nitrogen transports in a soil–paddy–atmosphere system using HYDRUS-1d and lysimeter experiment. *Paddy and Water Environment*, *15*(4), 831–846. https://doi.org/10.1007/s10333-017-0596-9

Jia, G., Shevliakova, E., Artaxo, P., Noblet-Ducoudré, N., Houghton, R., House, J., Kitajima, K., Lennard, C., Popp, A., Sirin, A., Sukumar, R., & Verchot, L. (2019). Chapter 2: Land-climate interactions (2019). *Climate change and land: An IPCC special report on climate change, desertification, land degradation, sustainable land management, food security, and greenhouse gas fluxes in terrestrial ecosystems.*

Jyotiprava Dash, C., Sarangi, A., Singh, D. K., Singh, A. K., & Adhikary, P. P. (2015). Prediction of root zone water and nitrogen balance in an irrigated rice field using a simulation model. *Paddy and Water Environment*, *13*(3), 281–290. https://doi.org/10.1007/s10333-014-0439-x

Kea, S., Li, H., Shahriar, S., Abdullahi, N. M., Phoak, S., & Touch, T. (2019). Factors influencing cambodian rice exports: An application of the dynamic panel gravity model. *Emerging Markets Finance and Trade*, *55*(15), 3631–3652. https://doi.org/10.1080/1540496X.2019.1673724

Kim, J., Park, H., Chun, J. A., & Li, S. (2018). Adaptation strategies under climate change for sustainable agricultural productivity in cambodia. *Sustainability*, *10*(12), 4537. https://doi.org/10.3390/su10124537

Kutilek, M., D.R., N., & K., R. (2007). Soil water retention curve, interpretation, 15.

LaHue, G. T., Chaney, R. L., Adviento-Borbe, M. A., & Linquist, B. A. (2016). Alternate wetting and drying in high yielding direct-seeded rice systems accomplishes multiple environmental and agronomic objectives. *Agriculture, Ecosystems & Environment*, *100*(229), 30–39. https://doi.org/10.1016/j.agee.2016.05.020

Lampayan, R. M., Samoy-Pascual, K. C., Sibayan, E. B., Ella, V. B., Jayag, O. P., Cabangon, R. J., & Bouman, B. a. M. (2015). Effects of alternate wetting and drying (AWD) threshold level and plant seedling age on crop performance, water input, and water productivity of transplanted rice in central luzon, philippines. *Paddy and water environment*.

Lehmann, J., Gaunt, J., & Rondon, M. (2006). Bio-char sequestration in terrestrial ecosystems – a review. *Mitigation and Adaptation Strategies for Global Change*, *11*(2), 403–427. https://doi.org/10.1007/s11027-005-9006-5

Li, Y., Šimůnek, J., Zhang, Z., Jing, L., & Ni, L. (2015). Evaluation of nitrogen balance in a direct-seeded-rice field experiment using hydrus-1d. *Agricultural Water Management*, *148*, 213–222. https://doi.org/10.1016/j.agwat.2014.10.010

Lim, T. J., Spokas, K. A., Feyereisen, G., & Novak, J. M. (2016). Predicting the impact of biochar additions on soil hydraulic properties. *Chemosphere*, *142*, 136–144. https://doi.org/10.1016/j.chemosphere.2015.06.069

Linquist, B. A., Anders, M. M., Adviento-Borbe, M. A. A., Chaney, R. L., Nalley, L. L., da Rosa, E. F. F., & van Kessel, C. (2015). Reducing greenhouse gas emissions, water use, and grain arsenic levels in rice systems. *Global Change Biology*, *21*(1), 407–417. https://doi.org/10.1111/gcb.12701

Liu, L., Chen, T., Wang, Z., Zhang, H., Yang, J., & Zhang, J. (2013). Combination of site-specific nitrogen management and alternate wetting and drying irrigation increases grain yield and nitrogen and water use efficiency in super rice. *Field Crops Research*, *154*, 226–235. https://doi.org/10.1016/j.fcr.2013.08.016

Lotse, E. G., Jabro, J. D., Simmons, K. E., & Baker, D. E. (1992). Simulation of nitrogen dynamics and leaching from arable soils. *Journal of Contaminant Hydrology*, *10*(3), 183–196. https://doi.org/10.1016/0169-7722(92)90060-R

Lu, S., Yu, X., & Zong, Y. (2019). Nano-microscale porosity and pore size distribution in aggregates of paddy soil as affected by long-term mineral and organic fertilization under rice-wheat cropping system. *Soil and Tillage Research*, *186*, 191–199. https://doi.org/10.1016/j.still.2018.10.008

Lüdemann, H., Arth, I., & Liesack, W. (2000). Spatial changes in the bacterial community structure along a vertical oxygen gradient in flooded paddy soil cores. *Applied and Environmental Microbiology*, *66*(2), 754–762. https://doi.org/10.1128/AEM.66.2.754-762.2000

Mambani, B., & Lal, R. (1983). Response of upland rice varieties to drought stress: I. relation between root system development and leaf water potential. *Plant and Soil*, *73*(1), 59–72.

McCullagh, P. (2019, January 31). *Generalized linear models* (2nd ed.). Routledge. https://doi.org/10.1201/9780203753736

Millington, R. J., & Quirk, J. P. (1961). Permeability of porous solids. *Transactions of the Faraday Society*, *57*(0), 1200–1207. https://doi.org/10.1039/TF9615701200

Mo'allim, A., Kamal, M., Muhammed, H., Mohd Soom, M., Mohamed Zawawi, M., Wayayok, A., & Che Man, H. (2018). Assessment of nutrient leaching in flooded paddy rice field experiment using hydrus-1d. *Water*, *10*(6), 785. https://doi.org/10.3390/w10060785

Monteith, J. L., & Unsworth, M. H. (1990). *Principles of environmental physics* (2nd ed). E. Arnold ; Distributed in the USA by Routledge, Chapman; Hall.

Moriasi, D. N., Arnold, J. G., Liew, M. W. V., Bingner, R. L., Harmel, R. D., & Veith, T. L. (2007). Model evaluation guidelines for systematic quantification of accuracy in watershed simulations. *Transactions of the ASABE*, *50*(3), 885–900. https://doi.org/10.13031/2013.23153

Mualem, Y. (1976). A new model for predicting the hydraulic conductivity of unsaturated porous media. *Water Resources Research*, *12*(3), 513–522. https://doi.org/10.1029/WR012i003p00513

Muhammad, N., Hussain, M., Ullah, W., Khan, T. A., Ali, S., Akbar, A., Aziz, R., Rafiq, M. K., Bachmann, R. T., Al-Wabel, M. I., & Rizwan, M. (2018). Biochar for sustainable soil and environment: A comprehensive review. *Arabian Journal of Geosciences*, *11*(23), 731. https://doi.org/10.1007/s12517-018-4074-5

Nabuurs, G.-j., Mrabet, R., Abu Hatab, A., Bustamante, M., Clark, H., Havlík, House, J., Mbow, C., Ninan, K., Popp, A., Roe, S., Sohngen, B., & Towprayoon, S. (2022). Agriculture, forestry and other land uses (AFOLU). *In IPCC, 2022: Climate change 2022: Mitigation of climate change. contribution of working group III to the sixth assessment report of the intergovernmental panel on climate change*. Cambridge University Press.

Nardi, P., Neri, U., Di matteo, G., Trinchera, A., Napoli, R., Farina, R., Subbarao, G. V., & Benedetti, A. (2018). Nitrogen release from slow-release fertilizers in soils with different microbial activities. *Pedosphere*, *28*(2), 332–340. https://doi.org/10.1016/S1002-0160(17)60429-6

Nash, J., & Sutcliffe, J. (1970). River flow forecasting through conceptual models part i — a discussion of principles. *Journal of Hydrology*, *10*(3), 282–290. https://doi.org/10.1016/0022-1694(70)90255-6

Phogat, V., Yadav, A. K., Malik, R. S., Kumar, S., & Cox, J. (2010). Simulation of salt and water movement and estimation of water productivity of rice crop irrigated with saline water. *Paddy and Water Environment*, *8*(4), 333–346. https://doi.org/10.1007/s10333-010-0213-7

Poulton, P. L., Vesna, T., Dalgliesh, N. P., & Seng, V. (2015). Applying simulation to improve rice varieties in reducing the on-fram yiled gap in cambodian lowland rice ecosystems. *Experimental Agriculture*, *51*(2), 264–284. https://doi.org/10.1017/S0014479714000271

Pratiwi, E. P. A., & Shinogi, Y. (2016). Rice husk biochar application to paddy soil and its effects on soil physical properties, plant growth, and methane emission. *Paddy and Water Environment*, *14*(4), 521–532. https://doi.org/10.1007/s10333-015-0521-z

Rassam, D., Simunek, J., Mallants, D., & Van Genuchten, M. (2018, August 1). *The HYDRUS-1d software package for simulating the movement of water, heat, and multiple solutes in variably saturated media: Tutorial*.

Resosudarmo, B. P., & Chheng, K. (2021). Irrigation inequality, rice farming productivity, and food insecurity in rural cambodia, 34.

Shekhar, S., Mailapalli, D. R., Das, B. S., & Raghuwanshi, N. S. (2017). Modelling water flow through paddy soils under alternate wetting and drying irrigation practice. *2017*, H43Q–07.

Shekhar, S., Mailapalli, D. R., Das, B. S., Mishra, A., & Raghuwanshi, N. S. (2021a). Hydrus-1d for simulating potassium transport in flooded paddy soils. *Communications in Soil Science and Plant Analysis*, *52*(22), 2803–2820. https://doi.org/10.1080/00103624.2021.1966437

Shekhar, S., Mailapalli, D. R., & Raghuwanshi, N. S. (2021b). Simulating nitrogen transport in paddy crop irrigated with alternate wetting and drying practice. *Paddy and Water Environment*, *19*(3), 499–513. https://doi.org/10.1007/s10333-021-00850-x

Shekhar, S., Mailapalli, D. R., Raghuwanshi, N. S., & Das, B. S. (2020). Hydrus-1d model for simulating water flow through paddy soils under alternate wetting and drying irrigation practice. *Paddy and Water Environment*, *18*(1), 73–85. https://doi.org/10.1007/s10333-019-00765-8

Šimůnek, J., Genuchten, M. T. v., & Å ejna, M. (2012). HYDRUS: Model use, calibration, and validation. *Transactions of the ASABE*, *55*(4), 1263–1276. https://doi.org/10.13031/2013.42239

Šimůnek, J., Šejna, M., Saito, H., Sakai, M., & Van Genuchten, M. (2013, January 1). *The hydrus-1d software package for simulating the movement of water, heat, and multiple solutes in variably saturated media, version 4.17, HYDRUS software series 3, department of environmental sciences, university of california riverside, riverside, california*.

Šimůnek, J., & Suarez, D. L. (1993). Modeling of carbon dioxide transport and production in soil: 1. model development. *Water Resources Research*, *29*(2), 487–497. https://doi.org/10.1029/92WR02225

Šimůnek, J., Van Genuchten, M. T., Jacques, D., Hopmans, J. W., Inoue, M., & Flury, M. (2018, September 11). 6.6 solute transport during variably saturated flow-inverse methods. In J. H. Dane & G. Clarke Topp (Eds.), *SSSA book series* (pp. 1435–1449). Soil Science Society of America. https://doi.org/10.2136/sssabookser5.4.c59

Singh, B. P., Fang, Y., Boersma, M., Collins, D., Zwieten, L. V., & Macdonald, L. M. (2015). In situ persistence and migration of biochar carbon and its impact on native carbon emission in contrasting soils under managed temperate pastures. *PLOS ONE*, *10*(10), e0141560. https://doi.org/10.1371/journal.pone.0141560

Singh, R., Dam, J., & Jhorar, R. K. (2003, December 31). Water and salt balance at farmers fields.

Sohi, S. P., Krull, E., Lopez-Capel, E., & Bol, R. (2010, January 1). Chapter 2 - a review of biochar and its use and function in soil. *Advances in agronomy* (pp. 47–82). Academic Press. https://doi.org/10.1016/S0065-2113(10)05002-9

Stolf, R., Thurler, Á. d. M., Bacchi, O. O. S., & Reichardt, K. (2011). Method to estimate soil macroporosity and microporosity based on sand content and bulk density. *Revista Brasileira de Ciência do Solo*, *35*, 447–459. https://doi.org/10.1590/S0100-06832011000200014

Suriya-arunroj, D., Chaiyawat, P., Fukai, S., & Blamey, P. (2000). Identification of nutrients limiting rice growth in soils of northeast thailand under water-limiting and non-limiting conditions. *Plant Production Science*, *3*(4), 417–421. https://doi.org/10.1626/pps.3.417

Tan, X., Shao, D., Gu, W., & Liu, H. (2015). Field analysis of water and nitrogen fate in lowland paddy fields under different water managements using HYDRUS-1d. *Agricultural Water Management*, *150*, 67–80. https://doi.org/10.1016/j.agwat.2014.12.005

Tuong, T. P., & Bouman, B. A. M. (2003). *Rice production in water-scarce environments* (IWMI Books, Reports H032635). International Water Management Institute.

Van Genuchten, M. T., Leij, F. J., & Yates, S. R. (1991, December 12). *The RETC code for quantifying the hydraulic functions of unsaturated soils* (Vol. 1.0). EPA Report 600/2-91/065.

Van Genuchten, M. T. (1980). A closed-form equation for predicting the hydraulic conductivity of unsaturated soils. *Soil Science Society of America Journal*, *44*(5), 892–898. https://doi.org/10.2136/sssaj1980.03615995004400050002x

Vereecken, H., Schnepf, A., Hopmans, J., Javaux, M., Or, D., Roose, T., Vanderborght, J., Young, M., Amelung, W., Aitkenhead, M., Allison, S., Assouline, S., Baveye, P., Berli, M., Brüggemann, N., Finke, P., Flury, M., Gaiser, T., Govers, G., ... Young, I. (2016). Modeling soil processes: Review, key challenges, and new perspectives. *Vadose Zone Journal*, *15*(5), vzj2015.09.0131. https://doi.org/10.2136/vzj2015.09.0131

Wang, K., Zhang, X., Sun, C., Yang, K., Zheng, J., & Zhou, J. (2021). Biochar application alters soil structure but not soil hydraulic conductivity of an expansive clayey soil under field conditions. *Journal of Soils and Sediments*, *21*(1), 73–82. https://doi.org/10.1007/s11368-020-02786-x

White, P. F., Oberthür, T., & Sovuthy, P. (1997). *The soils used for rice production in cambodia: A manual for their identification and management*. Int. Rice Res. Inst.

Witt, C., & Haefele, S. M. (2005, January 1). PADDY SOILS. In D. Hillel (Ed.), *Encyclopedia of soils in the environment* (pp. 141–150). Elsevier. https://doi.org/10.1016/B0-12-348530-4/00286-1

Xu, Y., Ge, J., Tian, S., Li, S., Nguy-Robertson, A. L., Zhan, M., & Cao, C. (2015). Effects of water-saving irrigation practices and drought resistant rice variety on greenhouse gas emissions from a no-till paddy in the central lowlands of china. *The Science of the Total Environment*, *505*, 1043–1052. https://doi.org/10.1016/j.scitotenv.2014.10.073

Yagi, K., Sriphirom, P., Cha-un, N., Fusuwankaya, K., Chidthaisong, A., Damen, B., & Towprayoon, S. (2020). Potential and promisingness of technical options for mitigating greenhouse gas emissions from rice cultivation in southeast asian countries. *Soil Science and Plant Nutrition*, *66*(1), 37–49. https://doi.org/10.1080/00380768.2019.1683890

Yagi, K., Tsuruta, H., & Minami, K. (1997). Possible options for mitigating methane emission from rice cultivation. *Nutrient Cycling in Agroecosystems*, *49*(1), 213–220. https://doi.org/10.1023/A:1009743909716

Yang, C., Yang, L., Yang, Y., & Ouyang, Z. (2004). Rice root growth and nutrient uptake as influenced by organic manure in continuously and alternately flooded paddy soils. *Agricultural Water Management*, *70*(1), 67–81. https://doi.org/10.1016/j.agwat.2004.05.003

Yang, R., Tong, J., Hu, B. X., Li, J., & Wei, W. (2017). Simulating water and nitrogen loss from an irrigated paddy field under continuously flooded condition with hydrus-1d model. *Environmental Science and Pollution Research*. https://doi.org/10.1007/s11356-017-9142-y

Yang, Y., Liu, B., Ni, X., Tao, L., Yu, L., Yang, Y., Feng, M., Zhong, W., & Wu, Y. (2021). Rice productivity and profitability with slow-release urea containing organic-inorganic matrix materials. *Pedosphere*, *31*(4), 511–520. https://doi.org/10.1016/S1002-0160(21)60001-2

Ye, Y., Liang, X., Chen, Y., Liu, J., Gu, J., Guo, R., & Li, L. (2013). Alternate wetting and drying irrigation and controlled-release nitrogen fertilizer in late-season rice. effects on dry matter accumulation, yield, water and nitrogen use. *Field Crops Research*, *144*, 212–224. https://doi.org/10.1016/j.fcr.2012.12.003

Zanutel, M., Garré, S., & Bielders, C. L. (2022). Long-term effect of biochar on physical properties of agricultural soils with different textures at pre-industrial charcoal kiln sites in wallonia (belgium). *European Journal of Soil Science*, *73*(1), e13157. https://doi.org/10.1111/ejss.13157

Appendices

A Incident on experimental columns

Figure 17: Gravity faith

B Soil profile

(a) (b)

Figure 18: Soil profile of the two soils

C Leaf area index measurement with the Petiole Pro app (version 1.4.15)

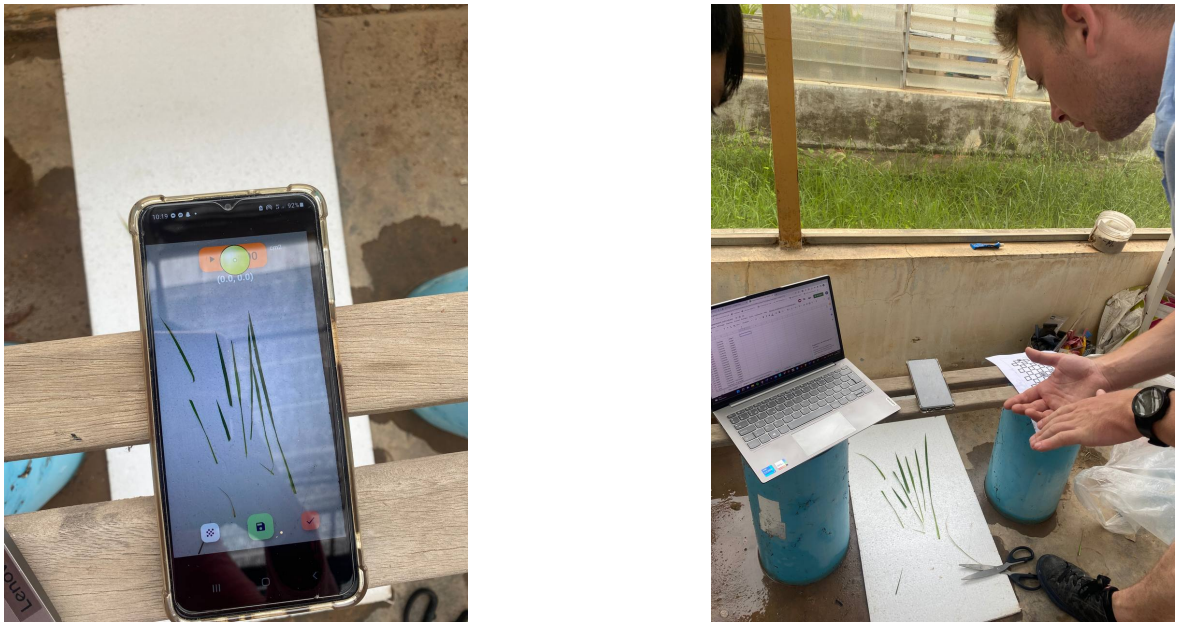

(a) (b)

Figure 19: Using of smartphone app to measure Leaf area index

D K_s handcrafted device

(a) (b) (c)

(d)

Figure 20: Handcrafted conductivity at saturation device. (a) sample ring, (b) constant head ring stick with a silicon joint, (c) excess water discharge spout, (d) final device with control overflow drip system to maintain a water constant head

E Calibrated parameters of Van Genuchten

Horizon	θ_R	θ_S	α	n	Ks	R^2
1 [0-20cm]	0,12	0,30	0,01	1,68	0,58	0,90
2 [20-40 cm]	0,10	0,34	0,02	1,33	29,75	0,86
3 [40-45cm]	0,20	0,33	0,01	1,67	38,04	0,82
1 + 4t/ha biochar	0,15	0,42	0,31	1,18	-	0,92
1 + 6t/ha biochar	0,16	0,42	9,33	1,07	-	0,93

Table 11: Van Genuchten parameters for Prateah lang soil (S1), calibrated from pressure plates experiment

Horizon	θ_R	θ_S	α	n	Ks	R^2
1 [0-10cm]	0,15	0,39	0,03	1,54	19,44	0,93
2 [10-25 cm]	0,16	0,25	0,00	1,57	38,04	0,69
3 [25-45cm]	0,18	0,41	0,10	1,50	3,24	0,89
1 + 4t/ha biochar	0,11	0,41	0,03	1,78	-	0,97
1 + 6t/ha biochar	0,14	0,33	0,01	2,84	-	0,90

Table 12: Van Genuchten parameters for Prey Khmer soil (S2), calibrated from pressure plates experiment

F Percolation volume comparison

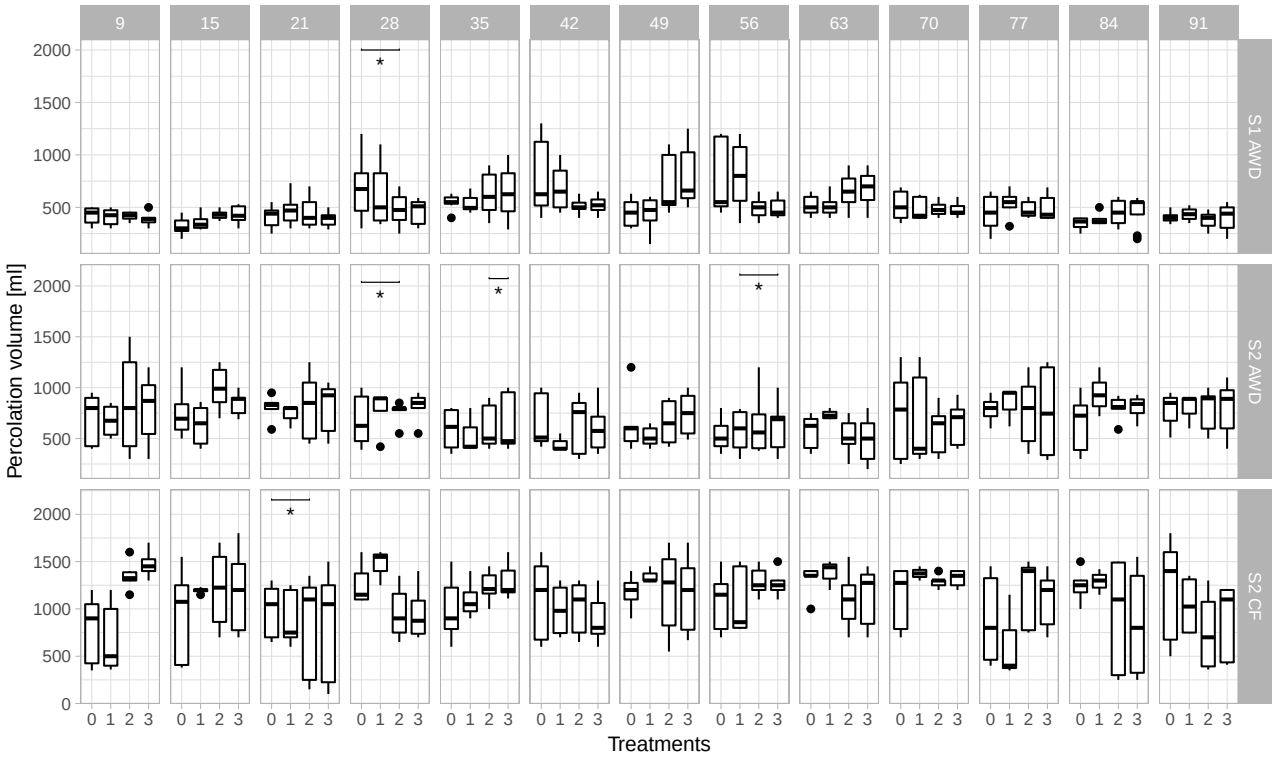

Figure 21: Comparison of percolation volume